Aalborg Universitet

AALBORG UNIVERSITY
DENMARK

Fundamental Study of Single Biomass Particle Combustion

Momenikouchaksaraei, Maryam

Publication date:
2013

Document Version
Publisher's PDF, also known as Version of record

[Link to publication from Aalborg University](#)

Fundamental Study of Single Biomass Particle Combustion

Maryam Momeni

Department of
ENERGY TECHNOLOGY E.T.

Fundamental Study of Single Biomass Particle Combustion

Maryam Momeni

Dissertation submitted to the Faculty of Engineering and Science in partial fulfilment of the requirementfor the degree of

DOCTOR OF PHILOSOPHY

Aalborg University
Department of Energy Technology
Aalborg, Denmark

to my family

Abstract

Maryam Momeni
2012

Fundamental Study of Single Biomass Particle Combustion

This thesis is a comprehensive study of single biomass particle combustion. The effect of particle shape and size and operating conditions on biomass conversion characteristics were investigated experimentally and theoretically.

The experimental samples were divided in two groups: particles with regular shapes (spheres and cylinders) and particles with irregular shapes (almost flake-like). A CAMSIZER analyser (Retsch Technology GMBH) was used to determine the size and shape of the particles via Dynamical Digital Image Processing. The experiments were performed in a single particle reactor under well-defined conditions, and the complete combustion processes were recorded as video sequences by a CCD camera installed in the set-up. One of the project objectives is to simulate conditions reasonably close to the conditions in a power plant boiler, i.e., reasonably high temperatures (up to 1600°C) and varying oxygen concentrations in the 5 to 20% range.

A one-dimensional mathematical model was used to simulate all the intraparticle conversion processes (drying, recondensation, devolatilisation, char gasification/oxidation and heat/mass/momentum transfer) within single particles of different shapes and size under various conditions. The model also predicts the flame layer domain of a single particle. The model was validated by experimental results under different conditions; good agreement between the model predictions and the experimental data was observed.

Both the experimental and modelling results showed that cylindrical particles lose mass faster than spherical particles of a similar volume (mass) and that the burnout time is reduced by increasing the particle aspect ratio (surface area to volume ratio). Very similar conversion times were observed for cylindrical particles with nearly identical surface area to volume ratios. Similar conversion times were also observed for two size classes of pulverised particles (with irregular shapes) made from the same type of wood because of their similar surface area to volume ratios. The ignition, devolatilisation and burnout times of particles were affected by the surrounding conditions (oxidiser temperature and oxygen concentration) to different extents, and the effect of oxygen concentration on the conversion time was more significant at lower oxidiser temperatures.

Acknowledgements

Three years studying in Aalborg University as a Ph.D fellow, with all its ups and downs, was one of the most valuable and exciting experiences, I've ever had. One of the joys of completion is to look over the journey past and remember all the friends and family who have helped and supported me along this long but fulfilling road.

First of all I would like to offer my deepest thanks to my supervisors, Professor Søren Knudsen Kær and Ascosiate Professor Chungen Yin at Aalborg University, for their kind guidance and assistance throughout these three years.

I would like to express my heartfelt gratitude to Dr. Søren Lovmand Hvid from DONG Energy, who was not only my external supervisor but real friend. Thank you Søren, for your great supervision, support, patient and encouragements. I learned a lot from you and this project could not be finished without your supports.

I also would like to appreciate Maja Bøg Toftegaard and Jimmy Andersen from DONG Energy for their participation in the project.

To the staff and students at Technical University of Denmark, and at Avedøre Power Plant, DONG Energy, I am grateful for the chance to visit and be a part of the lab. Thank you for welcoming me as a friend and helping to develop the ideas in this thesis.

I am very graitful to my colleagues in the department of Energy Technology, Alireza, Jessica, Christian, Erik, Samuel, Souman, Benoit, Vincenzo, Anders and Jacob for their support and for the great working environment they provide.

I would not have contemplated this road if not for my parents, Kourosh and Tahereh, and my siblings, Roya and Alireza who instilled within me a love of creative pursuits, science and language, all of which finds a place in this thesis. To my family, thank you, this thesis would also not be possible without your love and support.

And to my dear friends, Mahdi, Maryam (s) (Rahimi, Soleimanzadeh, Rashidi and Tahersima), Simin, Mehdi, Soroush, Mojtaba, Amin, Kamal, Behzad, Babak! thank you all! You have been like a family for me in the past three years! I never forget your supports and kindness ☺

Maryam Momeni
Aalborg, December 2012

List of publications

This dissertation is a collection of scientific papers based on the PhD project objectives set during the research work to advance scientific and industrial goals with consultancy of DONG Energy representatives. Most of the details of this research study are contained in the attached papers and therefore the presented manuscript should be intended only as an summary of the overall project.

This study is the outcome of my research as a PhD student at the Department of Energy Technology, Aalborg University, Denmark from October 2009 to September 2012. The work has resulted in two conference papers and three journal papers listed below:

Journal papers

Paper 1 Experimental study on effects of particle shape and operating conditions on combustion characteristics of single biomass particle. *Momeni, Maryam; Yin, Chungen; Kær, Søren Knudsen; Hansen, Troels Bruun; Jensen, Peter Arendt; Glarborg, Peter.* In Press, Energy&Fuels (2012)

Paper 2 A comprehensive study of ignition and combustion of single wooden particles. *Momeni, Maryam; Yin, Chungen; Kær, Søren Knudsen; Hvid, Søren Lovmand.* Under review, Energy&Fuels (2012)

Paper 3 Combustion of single pulverized biomass particle collected from a power plant under different operating conditions: Experimental and numerical studies**.** *Momeni, Maryam; Kær, Søren Knudsen; Yin, Chungen; Hvid, Søren Lovmand.* In Progress (2012)

Conference papers

Paper 4 Factors influencing the ignition and burnout of single biomass particle. *Momeni, Maryam; Kær, Søren Knudsen; Yin, Chungen; Hvid, Søren Lovmand.* 5th European Combustion Meeting, Cardiff (2011)

Paper 5 Experimental study of biomass particle combustion. *Momeni, Maryam; Kær, Søren Knudsen; Yin, Chungen; Hansen, Troels Bruun; Jensen, Peter Arendt; Glarborg, Peter.* 34th Symposium of combustion Institute, Warsaw (2012)

TABLE OF CONTENTS

LIST OF FIGURES

List of Tables

Thesis Outline

This dissertation is a collection of scientific papers based on the PhD project objectives that were set in consultation with DONG Energy representatives during the course of the research to advance scientific and industrial goals. The main body of the thesis consists of 6 chapters, which are described below.

Chapter 1
Introduction: An overview of the problems of climate change and fossil fuel depletion is presented, and motivation is provided for using biomass as a renewable energy source. The strategies used by power plants to switch from coal firing to co-firing with biomass and, recently, to pure biomass firing are also explained. The problem statement and the project motivation are described.

Chapter 2
Literature review: The specific targets of the current project are described, including single particle combustion and the effects of particle shape, size and operating conditions on the different stages of combustion, etc. Previous studies related to the project framework are reviewed. The novelty of the project and the differences between this work and previous studies are highlighted.

Chapter 3
Experimental work: Complete descriptions of the experimental set-up, test conditions and material preparation are given. The methodology of the work and the techniques used to analyse the results are described thoroughly. The limitations of the experimental study are also discussed.

Chapter 4
Modelling approach: The mathematical model is described in detail. The different steps of the particle combustion process are explained, and all the governing equations are presented. The criteria used to predict the different stages of particle combustion are discussed, and the implementation of the particle characteristics in the model is also explained.

Chapter 5
Results, discussions: The main results of the current project are summarised, including the experimental results, the modelling results and the validation. The results are divided into two groups: particles with regular shapes and particles with irregular shapes. The results summarised in this section are discussed comprehensively in the written papers attached to the end of the thesis.

Chapter 6

Conclusion and future works: The main conclusions of the current research project are also highlighted, along with the improvement in the accuracy of the results contributed by this work. At the end, the possibilities for improving the work in the future are also addressed.

<div align="right">

1

</div>

Introduction

An overview of the problems of climate change and fossil fuel depletion is presented, and motivation is provided for using biomass as a renewable energy source. The strategies used by power plants to switch from coal firing to co-firing with biomass and, recently, to pure biomass firing are also explained. The problem statement and the project motivation are described.

1.1. Climate change

Traditional fossil fuel-based energy sources effectively stimulate economic progress but also harm the environment.

Fossil fuel combustion releases various types of polluting gases, such as carbon dioxide, carbon monoxide, methane, nitrous oxide, etc., into the air. One of the more serious consequences of pollution caused by fossil fuels is global warming or climate change.

The released greenhouse gases act like a blanket around the Earth, trapping energy in the atmosphere and causing the atmosphere to warm. As a consequence of these issues and following the Kyoto Protocol greenhouse gas reduction targets, industrialised countries have been obliged to reduce greenhouse gas emissions by at least 5 % below 1990 levels over the period from 2008 to 2012. This obligation has led to an increased interest in research on renewable energy resources, such as biomass, wind, solar, hydropower, and geothermal energy, which are sustainable energy sources based on routinely available and indigenous resources.

1.2. Biomass as a renewable energy source

Biomass is the term used for all organic material of plant origin, which is essentially the collection and storage of solar energy through photosynthesis. Biomass energy, or bioenergy, is the conversion of biomass into useful forms of energy, such as heat, electricity and liquid fuels.

Biomass has provided energy for thousands of years and is still one of the most frequently used energy sources in the world. Biomass provides approximately 14% of the global energy supply [Balat and Ayar, 2005]. Biomass is an almost CO_2-neutral energy source, which means that plants absorb an amount of CO_2 during photosynthesis that is equal to the amount emitted when these plants are later used for energy production [Lu et al. 2010].

Furthermore, biomass has a lower content of sulphur and heavy metals than fossil fuels, which is better for the environment.

It should be noted that all biomass is not directly converted to energy but rather can be converted into intermediate energy carriers, which are named biofuels, such as charcoal (a higher energy density solid fuel), ethanol (liquid fuel), or producer-gas (from the gasification of biomass).
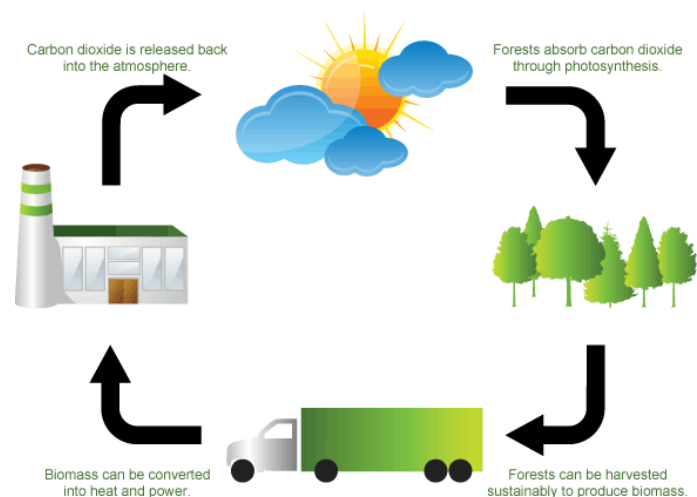
Figure 1. Biomass as a CO_2-neutral energy source [American Renewables, www.amrenewables.com]

"In Denmark, a country with significant amounts of land cultivation, biomass currently supplies approximately 70% of renewable energy consumption, mostly in the form of straw, wood and renewable wastes. The consumption of biomass for energy production in Denmark more than quadrupled between 1980 and 2005.

The biomass consumption is expected to further increase over the 2006 level (103 PJ). This expectation is primarily based on the 1993 policy agreement (the Biomass Agreement) and the February 2008 policy agreement on the increased use of straw and wood chips at large co-generation plants. Additionally, the consumption of biomass for heat production continues to rise in district-heating plants and in smaller installations for households, enterprises and institutions.

The global consumption of biomass for energy is estimated at approximately 50,000 PJ/year. This corresponds to approximately 12% of the total global energy consumption or approximately 80% of the global supply of renewable energy because wind power generates approximately 10,000 PJ/year, while other forms of renewable energy currently only provide a total of 2000-3000 PJ/year.'' [Danish Energy Agency, www.ens.dk]

1.3. Biomass co-firing

Co-firing is the simultaneous combustion of different fuels in the same boiler and provides an alternative for achieving emissions reduction [European Bioenergy Networks, www.eubionet.vtt.fi]. Biomass co-firing provides several benefits, such as avoidance of landfills and the associated costs, and reductions in sulphur oxide, nitrogen oxide, and greenhouse-gas emissions.

The NETBIOCOF project (2005-2007), which was co-financed by the European Commission, has reported in great depth on co-firing activities in Europe with regard to approximately 100 co-firing units. While the use of herbaceous biomass has created issues such as higher risks of slagging and fouling due to the higher inorganic matter content, positive results from using woody biomass have been reported. The chart below shows the division of co-firing plants across Europe. While many plants are in a trial or demonstration stage, the co-firing plants in the Netherlands, Denmark, Finland and Sweden are mostly operating on a commercial basis [European Biomass Industry Association, www.eubia.org].
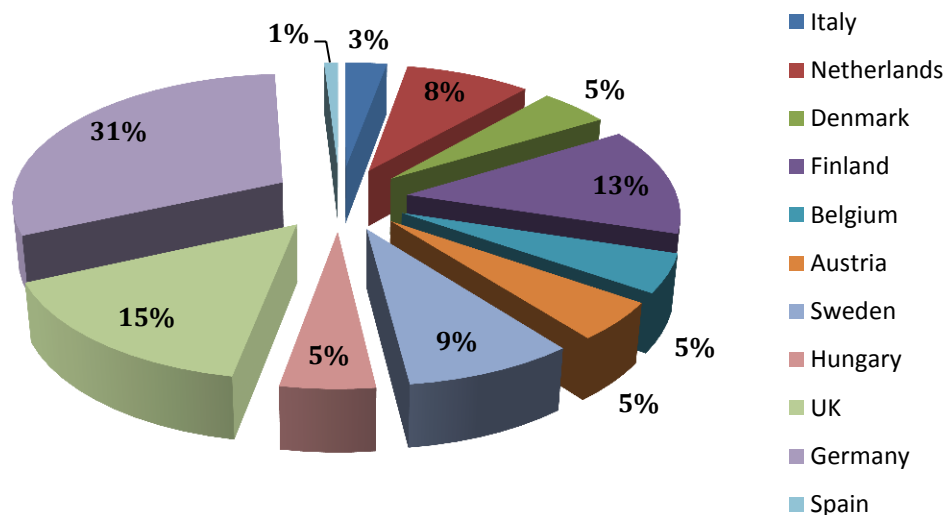
Figure 2. Co-firing power plants in Europe [European Biomass Industry Association, www.eubia.org]

Biomass firing is different from coal firing due to the wide variety of biomass sources and their different chemical and physical properties. This variation may have consequences for combustion plant behaviour, combustion stability, operational conditions and residues.

The milling process is a necessary pretreatment process to adapt particle physical and chemical properties to the requirements of different firing systems.

Particle size reduction is the main results of milling process which provides particles with higher density and larger surface area to volume ratio which cause to elevate chemical reactions. It also have drying effects and results in homogenization of particle physical properties [Mania et al. 2004, Esteban et al. 2006]. Different types of milling processes are applied in pulverized fuel burners such as hammer mill, roller mill, knife mill etc which result in particles with different characteristics.

Particle size

Biomass particles are typically much larger than pulverised coal particles. The average size of a pulverized coal particle is about 50 μm, whereas a biomass particle can be up to 200 times as large [Bharadwaj et al. 2004]. The large size of biomass particles has several effects on biomass combustion compared to traditional coal combustion.

The larger size of the biomass particle results in large internal gradients in the particle properties during reactions that are not found in pulverised coal. Thus, significant overlap between particle drying, devolatilisation, and oxidation processes may occur that considerably complicate the modelling of biomass conversion processes.

Larger particles also have a large boundary layer; thus, released volatile components can react with bulk gas components and result in significant thermal feedback to particles and correspondingly higher heating and reaction rates. Such considerations do not exist in small pulverised coal combustion.

Particle Shape

Depending on the type of mill used, biomass particles typically have irregular shapes with varying surface area to volume ratios. Most biomass particles are non-spherical and resemble cylinders or flakes. Pulverised coal particles can be approximated as spheres with aspect ratios of less than 2, while the aspect ratios for biomass particles commonly exceed 6 [Lu et al. 2011].

The irregular shapes of biomass particles result in more complex particle conversion behaviour than in coal combustion.

Large biomass particles commonly burn at or near diffusion-limited rates, so that the particle surface area to volume ratio plays a key role in the prediction of particle conversion times. The assumption of a spherical shape corresponds to using a minimum surface area to volume ratio in a biomass fuel conversion model which affects particle conversion rates.

Particle moisture content

Depending on the type of material, the time of harvesting, duration of storage and degree of pre-treatment, biomass fuels may have much higher moisture contents than typical coals. Moisture content affects the heating process and heat release and consequently burner flame stability.

Therefore, biomass fuel must be dried before combustion to be able to sustain combustion. The high fuel moisture content reduces the adiabatic combustion temperature so that biomass fuel needs a longer residence time in the combustion chamber to prevent emissions resulting from incomplete combustion and it also influences plant efficiency.

Particle composition

Biomass has a different chemical composition than coal. Biomass has higher fractions of oxygen and hydrogen and less carbon compared to coal, resulting in lower energy generation: about two-thirds as much as coal on a mass basis. Biomass also has a higher volatile content, resulting in predominantly gaseous combustion and lower char combustion. Table 1 summarises the chemical compositions of several important classes of fuels.
These parameters influence the optimum size and design of the combustion chamber and also affect the ideal flow rate of combustion air.

Table 1. Elemental analysis for several coal and biomass samples [Lu et al. 2011]

	Anthracite	Bituminous	Sub-bituminous	Lignite	Grass	Straw	Wood chips	Waste wood
C	90.22	78.35	56.11	42.59	45.34	48.31	51.59	49.62
H	2.85	5.75	6.62	7.40	5.82	5.85	6.14	6.34
N	0.93	1.56	1.10	0.73	2.04	0.78	0.61	1.01
O	5.03	11.89	35.31	48.02	45.95	44.18	41.57	42.89
S	0.96	2.43	0.84	1.15	0.24	0.18	0.07	0.07
Cl	0.03	0.08	0.01	0.01	0.62	0.70	0.02	0.06

Ash content

Coal typically has a higher ash content than biomass. Biomass ash contains relatively reactive salt compounds, while coal ash contains more stable silicates; thus, biomass ash is more disposed to form deposits in the combustor, which is known as slagging and fouling. Slagging and fouling can harm the combustor at high biomass mass fractions (~30%). However, low biomass mass fraction co-firing (~5 percent) makes no significant problems with the equipment [Ciolkosz 2010].
These types of differences cause the drying, devolatilisation, and oxidation time scales of millimetre-sized biomass particles to exceed those of pulverised coal particles under similar conditions and may affect heat release, emissions, boiler efficiency, ash deposition, and fouling in the reactor. Therefore, it is essential that the problems associated with biomass for co-fired and pure biomass-fired systems be managed to achieve more efficient and optimised boilers and burners.

1.4. Emissions

The greatest benefits of biomass compared to fossil fuels are associated with the reduction of CO_2 because biomass is considered to be CO_2-neutral. Additionally, biomass normally emits

less SO_x and NO_x than fossil fuels [Bioenergy for electricity and heat, report by DONG energy and VATTENFALL, 2007].

The emissions from biomass combustion depend on the composition of the biomass, the firing technology and the flue gas cleaning system.

As an example, dust emission in grate-firing is very low due to the removal of ash particles by a bag filter in flue gas cleaning. The S-, Cl- and N-contents of the biomass are partially converted to SO_2, HCl and NO_x, respectively, which are emitted with the flue gas. In straw firing, most of the S- and Cl-contents are captured to the ash as potassium sulphate and potassium chloride, respectively; only a small fraction of the N-content is converted into NO_x, while the rest is converted into N_2, which is already the main component of air [Bioenergy for electricity and heat, report by DONG energy and VATTENFALL, 2007]. Table 2 shows reported values from two different firing systems.

Table 2. Typical annual average emissions at 10% O_2 dry basis [Bioenergy for electricity and heat, report by DONG energy and VATTENFALL, 2007]

Emission	grate-fired wood chip plants mg/Nm^3	grate-fired straw plants mg/Nm^3
CO	75	200
SO2	5	100
HCl	-	50
NOx	150	200
Dust	10	10

1.5. Biomass combustion modelling

The performance optimisation of large utility pulverised fuel (PF) boilers has attracted much attention in recent years. Optimisation strategies are directed at extending boiler lifetimes and availability, increasing thermal efficiency and reducing pollutant emissions. Using biomass as a solid fuel introduces additional complications from devolatilisation behaviour and solids combustion compared to gas combustion. To achieve higher combustion efficiency, the major factors influencing (co-firing) PF systems should be investigated thoroughly; these factors include particle shape and size characteristics, gas and particle temperatures, ignition times and temperatures, local heat release, local oxygen concentration, kinetic parameters for devolatilisation and char oxidation and char properties. In engineering practice, it is very difficult to investigate the combustion processes of various types of combustibles directly in the boiler. Rather than constructing real boilers and attempting to measure and improve these characteristics, computers models are used to simulate boilers.

Combining computer modelling with experiments is a cost-effective approach for the design of biomass combustion applications and can improve the competitiveness of biomass combustion for heat and electricity generation. There are various types of modelling tools, such as simple heat and mass balance models, chemical equilibrium models, chemical kinetics models and, at a high user level, Computational Fluid Dynamics (CFD) tools. Computational fluid dynamics (CFD) modelling is an accurate and cost-effective tool that can provide insight into the combustion characteristics of unfamiliar fuels. Therefore, advanced CFD modelling is essential to optimise a firing system.

CFD modelling has been extensively applied to evaluate the combustion performance of fuels in bench, pilot and full scale furnaces [Yin et al. 2003, 2004 and 2010, Backreedy et al. 2005, Ma et al. 2009]. However, the multiphase combustion and different motion and conversion characteristics of biomass particles complicate solid fuel combustion modelling.

Thus, a great deal of research is being performed to improve the understanding of the fundamental processes of biomass combustion and to develop models that can be used effectively with CFD tools.

2

LITERATURE
REVIEW

The specific targets of the current project are described, such as single particle combustion and the effects of particle shape and size and operating conditions on the different stages of combustion, etc. Previous studies related to the project framework are reviewed. The novelty of the project and differences between this work and previous studies are highlighted.

Co-firing biomass with coal in existing power plants is an effective means of significantly increasing the proportion of renewable energy sources in the energy system and reducing CO_2 emissions that has been successfully demonstrated in over 200 power plants worldwide [IEA, http://www.ieabcc.nl/database/cofiring.php]. Nevertheless, fundamental combustion studies still must be conducted to determine combustion characteristics under well-controlled conditions and to aid in the design and operation of co-firing burners and boilers [Sami et al. 2001].

2.1. Single particle modelling

To predict the performance of different combustion systems, specific particle models need to be developed. The single particle model represents a well-defined system for fundamental studies on the interactions between chemical and physical processes.

Many experimental and modelling research studies have been performed on single particle combustion. The combustion process of a single particle involves many complex sub-processes, such as species diffusion, convective transport inside the particle, water evaporation and recondensation, secondary pyrolysis reactions inside the pores, shrinking and swelling, etc.; thus, assumptions and simplifications are needed to describe the various processes mathematically.

A single particle can be combusted in two different regimes: a thermally thick regime and a thermally thin regime. A thermal Biot number, which relates the internal and external heat transfer rates, determines the combustion regime:

$$Bi = \frac{l_c h}{k} \tag{1}$$

where l_c *(m)* is a characteristic length, h *(W/m^2 K)* is the convective heat transfer coefficient and k *(W/mK)* is the thermal conductivity of the particle. When $Bi <<1$, the resistance to heat transfer within the particle is small compared to the external heat transfer resistance, so that the particle is in the thermally thin regime. When $Bi >>1$, the particle is in the thermally thick regime, such that intra-particle temperature gradients exist and are important.

For small size particles, the Biot number is much smaller than one, and the assumption of an isothermal particle can be justified; however, larger biomass particles generally have Biot numbers that are larger than 1; for these particles, the isothermal particle assumption is not valid, and gradients exist within the particle that affect evaporation and devolatilisation rates, which are sensitive to the local solid temperature.

Solid fuel particles have short residence times in commercial boilers, which should be considered when contemplating the retrofit of an existing boiler for biomass combustion (either pure or co-firing); naturally, computational models for studying the boiler performance must also properly reflect the characteristics of the combustion process.

Most existing single particle models use a one-dimensional framework based on several assumptions (local thermal equilibrium, ideal gases, negligible kinetic, etc.); physical processes, such as heat transfer by convection, conduction and radiation, convective transport of volatile species, gas pressure and velocity variation, have been accounted for, and the effects of intra-particle heat and mass transfer on biomass heating and the devolatilisation rate have been studied in previous works [Di Blasi et al. 1996 and 2004, Larfeldt et al. 2000, Grønli et al. 2000, Bharadwaj et al. 2004, Porteiro et al. 2006, Lu et al. 2008, Sadhukhan et al. 2009].

Grønli et al. 2000 presented one dimensional modeling results of pyrolysis of single wood particle (d=20mm, l=30mm) under regimes controlled by heat and mass transfer .

They showed the importance of an accurate heat transfer model for prediction of intraparticle temperature profile throughout the pyrolysis process. In their study, a variable thermal conductivity as function of density, temperature and grain orientation and also including a radiant heat transfer term was suggested.

Larfeldt et al. 2000 modified one dimensional model of wood pyrolysis for a large particle (d=50mm , l=300mm). They showed that the inclusion of a shrinking model decreases the time of pyrolysis significantly.

Bharadwaj et al. 2004 studied the effects of intraparticle heat and mass transfer on the devolatilization process of millimeter-sized biomass particles. They presented a model which accounts for intraparticle heat and mass transfer during particle drying and devolatilization. Their results showed that the intra particle heat and mass gradient for large particle delay particle heating and devolatilization significantly. They presented that intraparticle effects delay the heating and devolatilization of a particle with 3mm diameter by several seconds compared to a lumped model's prediction.

Porteiro et al. 2006, presented a one dimensional mathematical model describing the thermal degradation of a large biomass particle (R=90mm). They used intra-particle combustion processes with extra-particle transport processes with thermal and diffusional control mechanisms in their model. The model was validated by experimental data in terms of particle mass loss and internal temperature.

Lu et al. 2008 developed a one dimensional model for a single biomass particle combustion. they showed that large temperature gradients exist in large particles during combustion. They compared the model predictions of near spherical particle (d=9.5mm) pyrolysis with isothermal and non-isothermal assumptions. The results indicated that the model with isothermal assumption predicts overall conversion rates approximately three times faster than the non isothermal model.

Sadhukhan et al. 2009 developed a mathematical model of large biomass particle pyrolysis. They included conductive and internal convection within the particle and convective and radiative heat transfer between the external surface and the bulk in the heat transfer model.

They investigated the effects of internal convection and particle shrinkage on particle pyrolysis and found to be substantially. They showed that it takes a significantly long period for surface temperature to reach the bulk temperature which emphasizes the the importance of including the external film heat transfer resistance in the model.

It is concluded from the results that the delayed conversion compared with a lumped model should be considered for commercial boiler with short residence time and should be accounted in computational models.

However, the majority of previous studies were performed for very large particles. Therefore, it is difficult to apply previous results to PF systems of millimetre sized (and even smaller) particles with rapid heating rates at high temperatures.

2.2. Thermal conversion of biomass

During the thermal conversion of biomass, a particle undergoes a variety of processes, such as drying, ignition, devolatilisation and volatiles combustion, char gasification and char oxidation. Depending on several parameters, such as the particle properties and the surrounding conditions, these processes can take place sequentially or simultaneously.

Drying

Moisture in a biomass particle can exist in two forms: free water and bound water. The fibre saturation point (FSP) criterion can be used to categorise moisture content, with an average value of 30% [Forest Products Laboratory United States Department of Agriculture Forest Service, 1999]; moisture content above the FSP is categorised as free water, whereas moisture content below the FSP is categorised as bound water. Free water exists as a liquid in the cells and pores of the particle, while bound water exists as moisture that is physically and chemically bound to surface sites and hydrate species. Free water vapourises from both the internal and external particle surface at a rate that is determined by the partial pressure of vapour in the gas phase, the surface saturated vapour pressure and the particle specific

surface area. However, the release of bound water is controlled by chemical reactions of the bound hydrates.

There are a large number of research studies that use drying models for biomass particles. Four basic models, including a thermal model, an equilibrium model, and a chemical reaction model, can describe wood drying under combustion heat fluxes [Bryden and Hagge, 2003].

Ignition

Particle ignition behaviour is not a basic property of fuels and depends on fuel properties and operating conditions; thus, the ignition behaviour of biomass is expected to be different from that of coal. Therefore, it is essential to conduct a detailed study on the ignition behaviour of biomass in relation to the biomass properties and the surrounding conditions to optimize combustion systems and to impede the formation of unburned residues and undesirable combustion conditions.

Many studies have been performed on solid fuel ignition. The ignition processes of coals have been investigated extensively [Abbas et al. 1994, Spliethoff et al. 1998, Sami et al. 2001, Damstedt et al. 2007, Lu et al. 2008], while biomass ignition behaviour and the effects of different factors on the ignition process have been studied both experimentally and numerically [Wornat et al. 1996, Liliedahl et al. 1998, Di Blasi et al. 1999, Kuo et al. 2005, Lu et al. 2008, Yang et al. 2008, Saastamoinen et al. 2010] under bed combustion conditions. The investigation of single particle combustion involves the fundamental study of both chemical and physical processes and their interactions under well-defined conditions. A few studies have investigated single biomass particle ignition experimentally and numerically. For instance, Grotkjær et al. 2003 investigated the ignition temperature of a single biomass particle by two different experimental methods: thermogravimetric experiments and pulse ignition experiments. The authors considered the ignition process to be initiated by oxidation on the particle surface. The authors also discussed that, as biomass particles contain a large amount of volatiles, both homogeneous and heterogeneous ignition can occur during particle combustion. For this reason, several different criteria were used to detect the ignition point during the experiments. Kuo and Hsi 2005 investigated the ignition of single wooden spheres heated in a hot air stream; the anisotropy of the thermal properties of the wood was found to have important effects on the ignition time of the wood, and different ignition modes (i.e., glowing ignition and flaming ignition) were observed. In Kuo and Hsi's study, the ignition modes and ignition criteria were neither interpreted nor discussed. Wang et al. 2009 investigated the combustion of biomass and biomass-coal blends by thermogravimetric experiments. The effects of cold moulding (a pelletisation method in which particles are compressed at temperatures of 70-80 °C) on fuel combustion were studied. Kinetic parameters and the ignition temperature were obtained by thermogravimetric analysis.

This literature review demonstrates that a limited amount of work has focused on single biomass particle ignition and in particular under conditions representative for large scale pf firing.

Devolatilisation

Much research has been conducted on biomass devolatilisation, and several mathematical models have been developed to describe the process.

In general, kinetic models of biomass devolatilisation processes can be categorised into three main groups:

- One-step reaction, successive reactions, or two-stage models;
- Chemical structure-based models; and
- Superposition models, which are based on the kinetics of individual components (cellulose, hemicelluloses and lignin) of the biomass.

Among these models, two-stage models that include the primary degradation of solids and the secondary degradation of primary pyrolysis products can be applied to simulate the devolatilisation process of biomass [Di Blasi, 1996a].

The yield of volatiles leaving the fuel particle surface during pyrolysis consists of a complex mixture that includes a large amount of hydrocarbons [Demyirbas 2003, Evans and Milne 1987a, Evans and Milne 1987b].

The distribution of devolatilisation products is known to depend on operational conditions, such as the heating rate, the reactor temperature, etc. [Demyirbas, 2003].

Volatile yields of several types of biomass under different conditions have been reported and can be used to model and analyse biomass devolatilisation [Ragland and Aerts 1991, Di Blasi 2000, Thunman et al. 2001, Grieco and Baldi 2011].

These types of information and modelling guidelines have been used in many research studies on the biomass devolatilisation process and investigations of the effects of different factors, such as particle properties and operational conditions, on the combustion process. Some recent works are discussed here.

Lu 2006 and Lu et al. 2008 and 2010 investigated the effects of particle shape and size on the devolatilisation of biomass particles. These authors studied three different shapes of different sizes: a near sphere, a cylinder and a flake. The large particles had an equivalent diameter of 9.5 mm and aspect ratios of 5 and 8; a cylindrical particle with an aspect ratio of 1 was assumed to be a sphere. The small particles had an irregular shape and an equivalent diameter of approximately 0.3 mm; the particle surface area and volume were measured and calculated using a 3-dimensional particle shape reconstruction algorithm based on three images taken from orthogonal directions. The calculation involved three major steps: image acquisition and processing, image contour alignment, and surface generation. Pyrolysis data collected from an entrained-flow reactor and a single particle reactor were reported. A one-dimensional, single particle devolatilisation model was also developed to simulate particles of different shapes and sizes.

Jiménez et al. 2008 performed devolatilisation and combustion experiments for pulverised biomass particles (~500 µm) in an entrained-flow reactor under realistic combustion conditions; useful Arrhenius parameters for the devolatilisation and combustion processes were derived.

Haseli et al. 2011 investigated the pyrolysis of a single biomass particle under a high heating rate. In this study, a one-dimensional model was used with the assumption that particle pyrolysis undergoes three parallel reactions that yield light gas, char and tar. Secondary reactions resulting in tar cracking to char and light gas were neglected. In the model, the heat of pyrolysis in the energy conservation equation was calculated by accounting for the exothermicity of char formation and the endothermicity of volatile generation using the correlations proposed in the literature. The model was validated by three sets of experiments and was used to investigate the effects of particle shape, size and initial density on conversion time. The authors also recommended using the kinetics data reported by Di Blasi and Branca 2011 for high reactor temperatures and the kinetics data reported by Thurner and Man 1981 for moderate rector temperatures.

Blondeau and Jeanmart 2011 developed a comprehensive model to investigate the pyrolysis of particles in pulverised flue boilers. The authors used a competitive, multi-component kinetics scheme, which was improved by using an additional char reaction at high temperatures. The authors derived apparent kinetic parameters from CFD simulations for eight spherical particles in the size range of 17 µm to 2.5 mm.

Char oxidation and Burnout

The chemical structure of biomass char is similar to that of coal char, but large physical differences exist between biomass char and coal char with regard to density, thermal conductivity, porosity, surface area, and particle shape and size.

Several fundamental studies have focused on the reactivity and conversion of single biomass particles or biomass char [Wornat et al. 1996, Liliedahl et al. 1998, Di Blasi et al. 1999, Lu 2006, Kuo et al. 2005, Lu et al. 2008, Yang et al. 2008, Jiménez et al. 2008, Biagini et al. 2009, Saastamoinen et al. 2010, Karlström et al. 2012]. For instance, Wornat et al. 1996 experimentally studied the combustion reactivity of chars produced from the pyrolysis of woody and herbaceous biomass and found that the pine and switch grass chars were quite reactive under conditions similar to those of pulverised fuel-fired boilers. The char burning rates were comparable to those of high-volatile bituminous coals in the early stages of char conversion and decreased to some extent as the reaction progressed.

Biagini et al. 2009 experimentally characterised the reactivity and morphology of biomass chars produced under high heating rates in a drop tube reactor. Karlström et al. 2012 determined the reaction orders and kinetic parameters for the oxidation of 5 anthracite chars and 1 biomass char at temperatures ranging from 1223 K to 1673 K using a multivariable optimisation method in which modelled burnout profiles were fitted to experimental data from a 4-m isothermal plug flow reactor operating at 10^4-10^5 K/s.

Mehrabian et al. 2012 developed a one-dimensional CFD model for the thermal conversion of thermally thick biomass particles. The authors described the spherical and cylindrical particles with a layer model, which was validated using the experimental data that Lu et al. 2008 obtained from a single particle reactor. In the validation, quite large cylindrical particles with diameters of 9.5 and 6.35 mm and moisture contents of 6% and 40% were selected. Centre and surface temperatures and the mass loss history of the particles were reported and validated.

Haseli et al. 2011 presented a one-dimensional model for the combustion of a single biomass particle. The authors validated their model for spherical particles with diameters of 1 and 10 mm using two sets experimental data from the literature. The authors reported conversion times for particles of different sizes at different temperatures. The authors also concluded that the gas phase combustion in the boundary layer for small particles and at high temperatures could be neglected.

Yang et al. 2008 numerically studied the effects of particle size in terms of mass loss history, maximum and minimum temperatures and individual process rates on the combustion characteristics of single biomass particles in the 10 μm to 20 mm size range.

The authors concluded that in a PF furnace, the transition from thin to thick particles takes place for spherical particles that are 200–250 μm in diameter and for cylindrical particles that are 150–200 μm in diameter, depending on the exact heat transfer conditions.

2.3. Biomass co-firing and pulverised fuel combustion

Ma et al. 2007 presented a CFD model for predicting the combustion of single wooden particles in a PF furnace. Particles with a mean size of 0.33 mm and a shape factor of 0.25 were assumed to be isothermal. The authors concluded that the particle shape had a significant effect on the particle trajectories, residence time and ash deposition characteristics. The authors also mentioned that biomass char is much more reactive than coal char. This result is because biomass particles mainly maintain their original irregular shape during devolatilisation, which leads to a higher surface area for biomass char and a larger oxygen flux into biomass char and contributes to a much higher char combustion rate compared to that of spherical coal particles.

Gera et al. 2002 studied the effects of the large aspect ratio of biomass particles on carbon burnout in co-firing switch grass and coal. The authors indicated the importance of the shape factor in specifying a suitable sizing criteria for a biomass processing scheme in co-firing applications. Traditional sieving and classification equipment is typically based on one-dimensional considerations; however, the specification of a 6-mm top size particle would be expected have a large aspect ratio based on the types of shredding/grinding equipment available and could be suitable for co-firing applications in a boiler, while a smaller size class should be considered to be more spherical in shape.

Yin et al. 2010 used CFD to model the co-firing of wheat straw with coal in a 150 kW swirl-stabilised dual reactor. The authors used a 1D model to simulate the particle conversion of particles that were a few hundred microns in diameter. In this study, both the coal and straw particles were assumed to be spherical and isothermal due to their small size; sub-processes occurred sequentially in the study.

Saastamoinen et al 2010 modelled the burning of coal and biomass particles at different oxygen concentrations (5 and 10%) and different temperatures (1173, 1373 and 1573 K); the results were compared to measurements in an entrained-flow reactor. The authors also studied the burning of pulverised biomass in a large-scale utility boiler. A single particle model was applied to calculate the burnout in the boiler. The authors concluded that the biomass particle size could be much larger than that of coal to reach complete burnout due to

the lower density and greater reactivity of the biomass particles. In this model, the biomass and coal particles were assumed to be spherical, with diameters in the 0.5 to 4 mm range.

Li et al. 2012 studied a torrefaction-based co-firing system experimentally and numerically. Torrefied biomass was used as a modified biomass with higher energy density, good grindability, higher flow ability and more uniformity in product quality than typical biomass. A CFD model was developed for a torrefaction-based co-firing system in a pulverised coal boiler aimed at 100% fuel switching. Different cases were simulated for pure coal and for biomass concentrations from 25 to 100%, with particle sizes in the range of 62-150 μm. The results showed that torrefaction is a viable technical option for high biomass replacement in a co-firing system, and no evidence was found indicating a reduction in the energy efficiency or fluctuations in the boiler load.

Gubba et al. 2012 developed a CFD model for the co-firing of coal and wheat straw at two biomass loadings (6% and 12%) in a 300 MWe tangentially fired furnace. The authors accounted for the internal heat transfer within the wheat straw particles in the model. The biomass particle size was less than 1.5 mm, and the particle aspect ratios were in the range of 1 to 3. Particles with an aspect ratio of 1 were assumed to be spheres, whereas those with a larger aspect ratio were considered to be cylinders.

All of these experimental and numerical works provide very valuable insights into the overall combustion and emissions from biomass flames or co-firing flames, as well as the fundamental conversion and reactivity of single biomass or biomass char particles. However, the number of these fundamental characterisations of biomass particle conversion and biomass co-firing flames is still severely limited.

2.4. Problem Background

In addition to the great diversity in the physical and chemical properties of biomass, raw biomass particles are often fibrous and non-friable and are, therefore, difficult to pulverise to a similar size as coal particles. For example, the sizes and shapes of pulverised biomass particles in commercial suspension co-firing consist of highly non-spherical milled biomass particles with a mean length of more than 15 mm and a maximum length of more than 100 mm. However, biomass is more commonly prepared for suspension co-firing in the latest retrofits (e.g., in Amager unit 1 in Denmark) by first pelletising the raw biomass and then separately pulverising biomass pellets in traditional coal mills or hammer mill trials, followed by pneumatic transportation to burners. The new process results in somewhat smaller biomass particles than the previous process. The new process still produces non-spherical particles with a maximum size of a couple of millimetres.

Determining the exact shape and size of such small particles to estimate the particle surface area and volume presents a challenge in modelling and analysis. In most previous work, the exact particle shape was determined only for quite large particles, whereas small particles were mainly assumed to be spherical. The pulverised biomass particles that are used in PF boilers are non-spherical and appear more as flakes or cylinder-like particles. A literature review shows that limited work has focused on biomass combustion using realistic sizes and shapes under conditions similar to PF boilers that need special attention in retrofitting and on the optimisation of the original burners for co-firing [Mandø et al. 2010, Yin et al. 2010].

2.5. Project Objectives

The objective of this project is to develop experimental and modelling descriptions of single particle combustion under different conditions relevant to industrial pf firing. The knowledge and capability gained from this project are used to understand and improve the combustion characteristics of industrial biomass suspension co-firing or pure biomass firing. This overall objective includes the following experimental and theoretical goals:

- Establish a comprehensive database including the ignition, devolatilisation and burnout times of single biomass particles of various shapes and sizes under different operating conditions;

- Further develop an existing comprehensive particle combustion model by including particle drying, devolatilisation, char gasification and oxidation processes. The model should account for the effects of particle shape and size, oxidiser temperature, oxygen concentration, etc.

2.6. Approach

The objectives of this project are achieved by completing the following tasks:

- *Particle size and shape analysis*

  Cylindrical and spherical particles (regular shapes) with different sizes and aspect ratios are made from pine wood; the particles are measured by caliper with a resolution of 0.05 mm.
  Particles with irregular sizes and shapes are analysed by a CAMSIZER, which is an opto-electronic instrument that measures particle sizes in the 30 μm to 30 mm range using Dynamical Digital Image Processing.

- *Single particle reactor*

  The experiments are conducted in a single particle reactor located in the CHEC/DTU laboratory. The particles are combusted at temperatures in the 1200°C to 1600°C range with oxygen concentration levels in the 5 to 20% range. A CCD camera is used to record the entire combustion process, and the particle combustion data are collected as video sequences. Selected tests are repeated 3 to 5 times to ensure the reproducibility of the results.

- *Data collection and analysis*

  A single particle reactor is used in this project to determine ignition, devolatilisation, and burnout times of single biomass particles under different conditions.

Specific criteria are applied to detect and estimate the ignition, devolatilisation and burnout times from images recorded by the CCD camera.

- *Development of a comprehensive solid/droplet particle combustion model*

A one-dimensional mathematical model is developed to investigate the conversion process of a single particle under different conditions. The model is able to simulate all the intraparticle conversion processes (drying, recondensation, devolatilisation, char gasification/oxidation and heat/mass/momentum transfer) for single particles of various shapes under different conditions. A mass and heat transfer coupled model is used to simulate the evaporation and recondensation of moisture for the particle, and a two-step global schematic model describes the biomass devolatilisation kinetics.

A simple mass transport model is used to describe biomass char oxidation. Oxidation kinetic processes are included in the model with some simplifying assumptions.

The intraparticle conversion processes for a single particle are modelled based on the three sub-models discussed above. The predictions of the model are validated by the experimental results.

3

EXPERIMENTAL WORK

Complete descriptions of the experimental set-up, test conditions and materials preparation are given. The methodology of the work and the techniques used to analyse the results are described thoroughly. The limitations of the experimental study are also discussed.

3.1. Experimental set-up

The experiments were performed in the single particle combustion reactor shown in Figure 3 and 4. The setup is located in the laboratory of the CHEC group at the Technical University of Denmark. Parameters such as the gas temperature, the oxygen concentration and the air velocity are controllable in the set-up so that the burning of fuel particles occurs under well-defined conditions. The utilised conditions are similar to those of high temperature suspension-fired boilers.

The set-up is placed in a fume hood to ensure the safe and complete removal of the flue gases by the ventilation system. The use of a fume hood necessitates the attachment of a heat shield to the top of the reactor to protect the fume hood by absorbing and dissipating the heat from the hot flue gas leaving the reactor. As shown in the figures, the set-up is equipped with a small rectangular mirror that is placed between the top of the reactor and the heat shield. The mirror can be pointed down towards the burner to observe the behaviour of the flame during combustion.

The set-up mainly consists of a reactor, a burner, a safety system and a gas supply system. A more detailed description of the different parts of the set-up is given in the following section.

Figure 3. Frontal view of the set-up

Figure 4. Left-side view of the set-up

Combustion Reactor

The reactor is a cylindrical vertical reactor with a height of 50 cm, which includes an inner ceramic tube with a diameter of 5 cm that is enclosed by isolating material.

The ceramic tube is made of aluminium oxide that can withstand the high temperatures resulting from combustion inside the reactor. Due to the relatively high thermal conductivity of aluminium oxide, isolation is necessary to prevent heat losses to the surroundings and to decrease the temperature gradient across the reactor cross-section. The tube is isolated by Skamol V-1100 with a thickness of approximately 10 cm. Additionally, all the holes in the tube can be closed by blank clamps to prevent atmospheric air from entering into the reactor. These clamps are necessary because the entering atmospheric air may affect the temperature and oxygen concentrations in the combustion zone.

The details of the reactor dimensions and the locations of the reactor components are shown in Figure 5 and Figure 6.
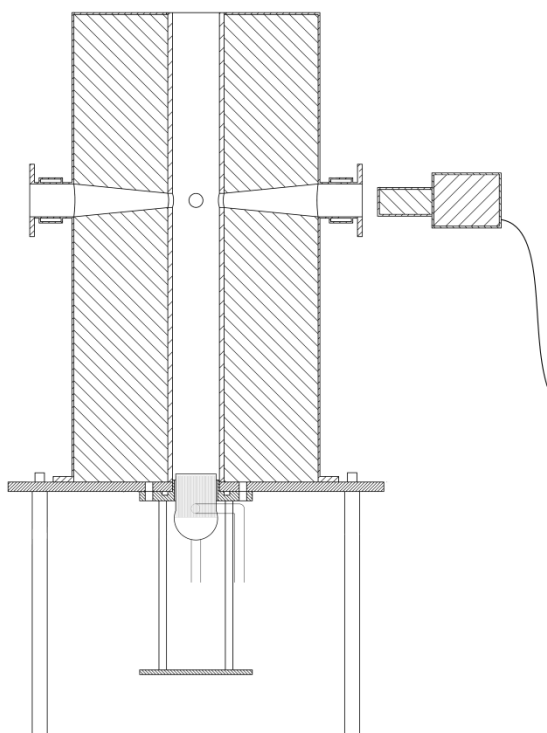
Figure 5. Schematic of the experimental set-up
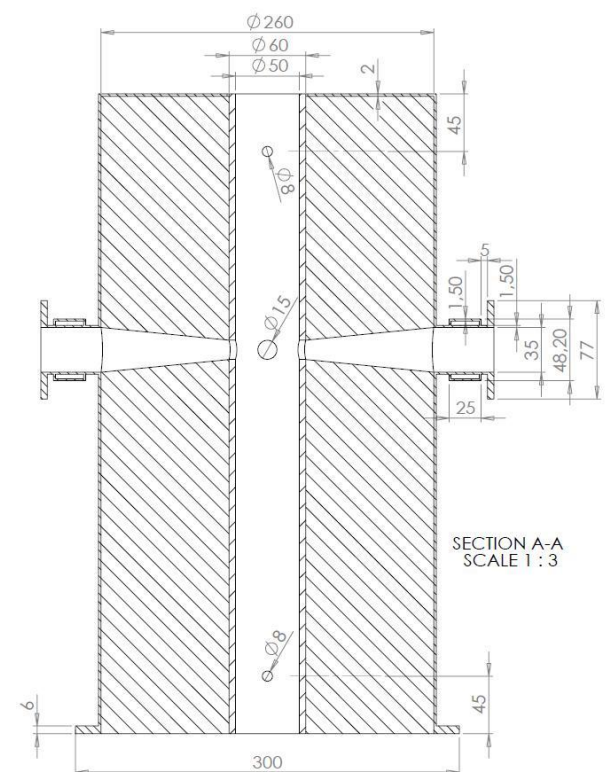
Figure 6. Detailed 2D drawing of the reactor with dimensions given in mm

Glass Burner

The burner is a Blue Flame Technology 94 Jet Burner made of quartz glass. The number 94 in the burner name refers to the 94 nozzles from which gases can be introduced at the top of the burner. The large number of injection nozzles (94) and the flat burner profile result in a desirable mixture of gases, an efficient gas flow distribution through the reactor and a flat temperature profile. The burner is shown in Figure 7. Inlet 1 directs the gas through the nozzles, and inlet 2 supplies the gas to the top of the burner through the nozzles.

The burner is supplied by liquefied petroleum gas (LPG) (a mixture of propane (~ 90%) and butane) and nitrogen via inlet 1 and a mixture of nitrogen and oxygen via inlet 2. The velocity of each gas is individually controlled, while the flame size can be controlled by regulating the injection of N_2 and O_2.

Figure 7. Quartz glass burner with two inlets

Mass Flow Control

The flow rates are controlled by 5 mass flow controllers (MFCs) of the EL-FLOW type with capacities ranging from 6.8-140 Nl/min; the controllers are connected to a computer. LabVIEW 8.6 software is used to regulate and control the flow rates. The change in and the stabilisation of the flue gas temperature is measured using an N-type thermocouple that is monitored in LabVIEW 8.6. Monitoring determines when the temperature inside the reactor has stabilised so that the experiments can begin.

Camera

The entire combustion process is recorded by a high performance camera. The camera is an Allied Vision Technologies Stingray F-033 that can record 65 images per second on average. The frame rate can be increased or decreased by changing the image size and the shutter time. The camera is connected to a computer, and AVT SmartView 1.11 software is used to regulate and edit the image settings. The captured images are then converted to an AVI video by a Matlab script. The camera is located in the back of the reactor, and the combustion is viewed through an observation hole. Figure 8 shows the camera and its position in the experimental set-up.

Figure 8. The CCD camera

Suction Pyrometer

The temperature of the flue gas inside the reactor is measured by a suction pyrometer. The pyrometer consists of an S-type thermocouple, which is surrounded by two concentric aluminium oxide tubes that minimise the thermal effects of radiation from the surrounding surfaces and the flame. High temperature flue gases are sucked in by a vacuum pump with a condensate separator at a volumetric flow rate of 3 l/min at 4 °C.

3.2. Materials

The materials used in the experiments are classified in two groups: regularly shaped particles and irregularly shaped particles. More detailed information on both groups of particles is presented in the following sections.

1. Regularly shaped particles

The investigated fuel is a low ash-content pine wood supplied by FLSmidth; the ultimate and proximate analysis of the fuel is given in Table 3.

The wooden particles investigated are 3 mm-diameter spheres and cylinders of varying aspect ratios (AR=length/diameter =2, 4, 6 and 8). The sample dimensions were measured by calibre to an accuracy of 0.05 mm. All the samples, both spherical and cylindrical, are produced with the same mass or volume but have different shapes (i.e., different aspect ratios).

Table 3. Chemical analysis of the pine wood used in the experiments

Ultimate (as received (ar), wt. %)		*Proximate (as received (ar), wt. %)*	
C	45.8	Dry loss	9.3
H	5.95	Ash	0.3
N	0.03	Volatiles	77.4
O	47.92	Fixed carbon	13
Density (kg/m^3)	600	NCV (kJ/kg)	16982.5

A small hole is drilled through the prepared samples, and a 0.35 mm platinum wire is threaded through a hole in the particle. Figure 9 shows the entire preparation procedure for a cylindrical particle.
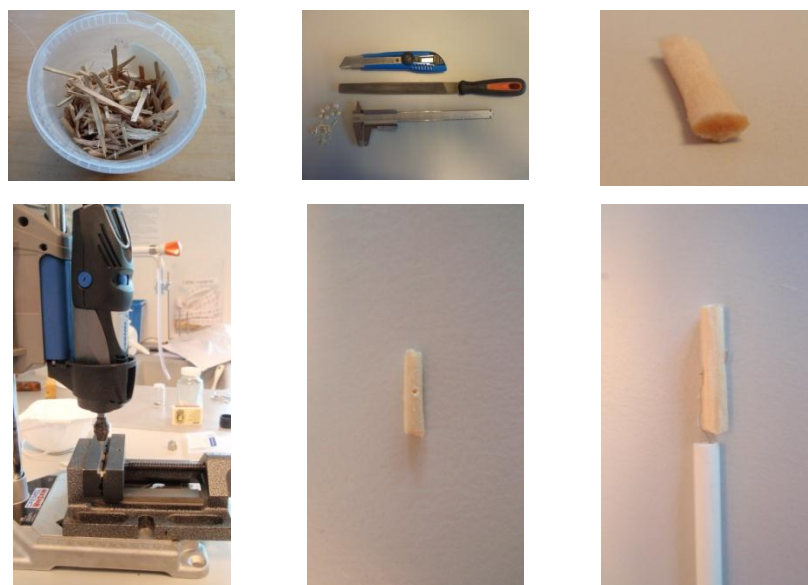

Figure 9. Sample preparation procedure

The three different cylindrical particles have similar diameters (3 mm) but have different lengths and, correspondingly, different volumes. All the regularly shaped samples are weighed using a digital scale with an accuracy of 10^{-5} g before testing; there is less than a 5% difference in the sample weights. Table 4 shows all the sizes, shapes and average masses for the particle samples, and Figure 10 shows images of the prepared particles of different shapes and sizes.

Table 4. Sample size and shape characteristics

Shape	d (mm)	L (mm)	AR	M (g)	S/V (mm^{-1})
Sphere	3.0	-	1	≈ 0.0125	2.0
Cylinder	2.08	4.16	2	≈ 0.0125	2.4
Cylinder	1.65	6.60	4	≈ 0.0125	2.7
Cylinder	1.44	8.65	6	≈ 0.0125	3.0
Cylinder	1.31	10.48	8	≈ 0.0125	3.2
Cylinder	3.0	6	2	0.0230	1.6
Cylinder	3.0	12	4	0.0490	1.5
Cylinder	3.0	18	6	0.0695	1.4

Spherical particle d_p=3 mm

Cylindrical particles AR=2, 4, 6, 8

Cylindrical particles d_p=3 mm L=6, 12, 18

Figure 10. Regularly shaped samples

2. Irregularly shaped particles

The irregularly shaped particles investigated were collected at the Avedøre power plant unit 2 (DONG Energy). The samples fall into two groups: samples from the hammermill trials and samples after the coal mill at the Avedøre power plant.

The pellets from the hammermill trials are delivered from either Kolding or Ålborg. The 6 mm-pellets are made from coarse particles and are delivered from Kolding, while the 8 mm-pellets were made of fine particles and are delivered from Ålborg.

The samples after the coal mill simply represent what is inside the silo at the time of collection. The origin of the pellets is not known, as pellets from many different

suppliers are mixed in the silo. The samples are separated into two size classes (2 and 3 mm) by sieving. Figure 11 Figure 12 show the two groups of samples.
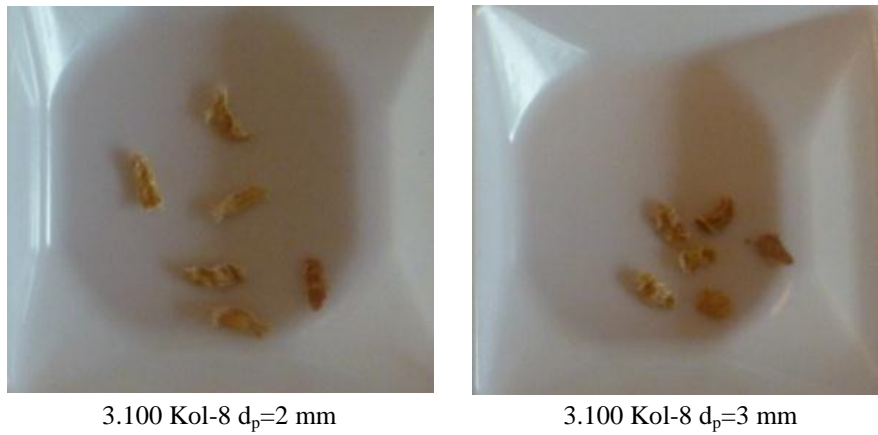

3.100 Kol-8 d_p=2 mm	3.100 Kol-8 d_p=3 mm

Figure 11. Samples from hammermill trials

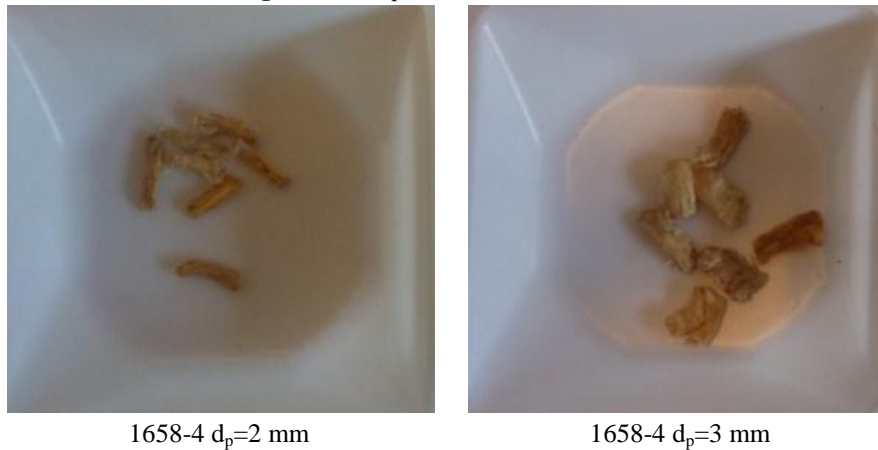|	
1658-4 d_p=2 mm	1658-4 d_p=3 mm

Figure 12. Samples from rollermill trials

The actual particle density of the samples is measured by ethanol displacement method at the Avedøre power plant laboratory to be approximately 1300 kg/m^3, as shown in Table 5.

Table 5. Sample densities

	Hammermill	Density g/ml		Coal mill	Density g/ml
1	7.6 ÅLB-2 1663-10	1.287	7	1658-9	1.324
2	6.60 ÅLB-5 1663-9	1.259	8	t-8591	1.314
3	8.100 ÅLB-6 1663-14	1.305	9	1658-12	1.28
4	8.60 ÅLB-10 1663-6	1.305	10	1658-4	1.287
5	3.100 KOL-8 1663.18	1.305	11	1658-10	1.324
6	4.60 KOL-9 1663-4	1.285	12	1657-4	1.296

These samples are drilled similarly to the regularly shaped samples so that they can be attached to a probe for insertion into the reactor. Figure 13 shows how the particle is held fixed prior to being drilled.

Figure 13. Particle held fixed for drilling

The particle size data from the power plant are based on sieving, which is not sufficiently accurate for comparisons or implementation in the model. Thus, many more details are needed. In this study, the particle sizes and shapes are measured by a CAMSIZER analyser, which is an opto-electronic instrument for measuring sizes in the 30 μm to 30 mm range. The measurements are based on Dynamical Digital Image Processing. The basic units of the CAMSIZER for analysing the shape and size characteristics of the particle samples include a dosage funnel, a dosage feeder, a planar illumination unit, a measurement shaft, an electronic assembly, a camera CCD basic, a camera CCD zoom and a sample collection unit. Figure 14 shows a schematic of the CAMSIZER.

Figure 14. Schematic of the CAMSIZER

The samples are supplied to the device either manually or automatically through the storage funnel. The samples are transported through the dosage feeder to the measurement area. The quantity of samples falling into the measuring area is controlled by adjusting the height of the funnel and the vibrational amplitude of the feeder, which are both controlled by computer. The CCD cameras are located opposite a planar illumination unit to guarantee optimum illumination of the image scene. The images of samples in the size range of 300 μm-30 mm are captured by the

CCD basic camera, and those of particles in the size range of 30 μm-3 mm are captured by the CCD zoom camera. The frame rate is approximately 60 images/sec. All the device functions for the measurement process and analysis are controlled by the CAMSIZER analysis software, which is installed on the computer. Figure 15 shows the particle images captured by the CAMSIZER.
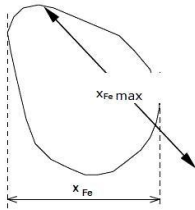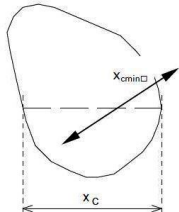

Figure 15. Particle images captured by the CAMSIZER

The software analyses the particle shape and size from the captured images by calculating various defined parameters. All the parameters used in this study are reported in Table 6. For example, Figure 16 shows statistics for the particle length ($X_{Fe, max}$ in mm and X_{length} in mm) and the particle diameter ($X_{Fe, min}$ in mm and $X_{c, min}$ in mm) for 3.100 KOL-8 (hammermilled samples); these parameters are measured by the CAMSIZER for several samples.

The particle mass is measured using a digital scale with an accuracy of 10^{-4} g, and the exact particle volume is calculated from the measured particle density and mass.

Table 6. Parameters describing particle size and shape

|		
X_{Fe}	Feret Diameter: distance between two tangents perpendicular to the measuring direction. $X_{Fe\ max}$ and $X_{Fe\ min}$ are the longest and shortest Feret diameters, respectively.	
X_C	Maximum chord of a particle projection in the measuring direction. $X_{c\ min}$ is the shortest chord in the measured set of maximum chords	
X_{area}	Diameter of an equivalent circle with a similar area as the particle projection area.	$X_{area}=(4A/\pi)^{\frac{1}{2}}$
X_{length}	Particle length, which is calculated from the maximum Feret diameter and the smallest chord of the particle projection.	$X_{length}=(X_{Fe\ max}{}^2-X_{C\ min}{}^2)^{\frac{1}{2}}$
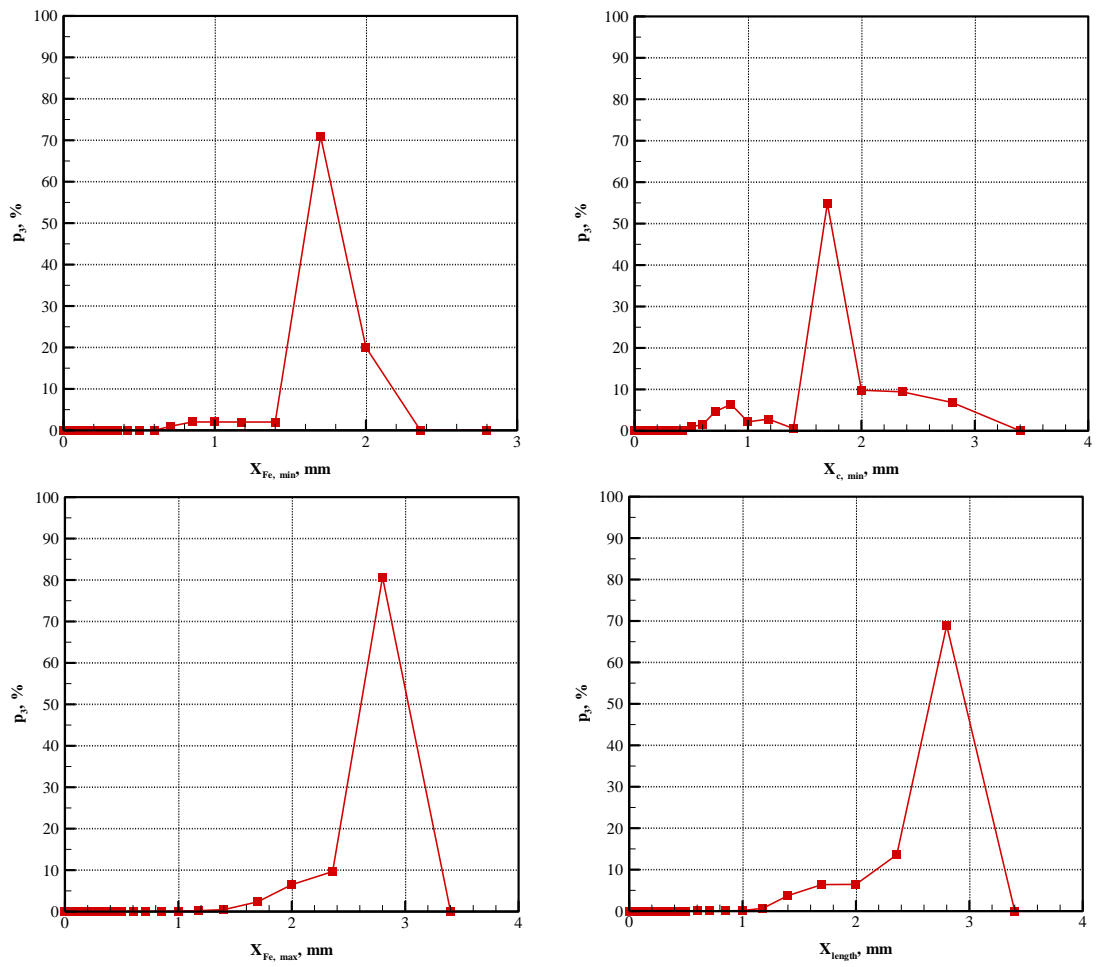
Figure 16. Statistical measurements of particle dimensions (length and diameter)

The CAMSIZER also approximates the sample particles as disk-shaped particles of a similar surface area to the actual samples by particle projection and reports the simulated disk diameter (X_{area}). Figure 17 shows a schematic of the estimation process. The aspect ratio is determined from the particle volume and the estimated surface area by assuming that the particle is a circular disc of thickness t, where the aspect ratio is defined as X_{area}/t. The particle thickness is calculated by V/A and is validated by the direct measurements by calliper.
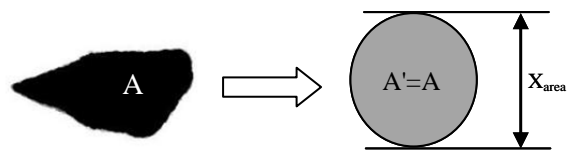

Figure 17. X_{area} estimation by the CAMSIZER

A thin flake-shaped particle can be presumed to be a disk for modelling purposes, so the CAMSIZER estimation enables accurate assumptions to be made about the surface area and the aspect ratio of the particle. Figure 18 shows statistics for the estimated X_{area} for

3.100 KOL-8 that correspond to a length and diameter of approximately 2.8 mm and 2 mm, respectively.
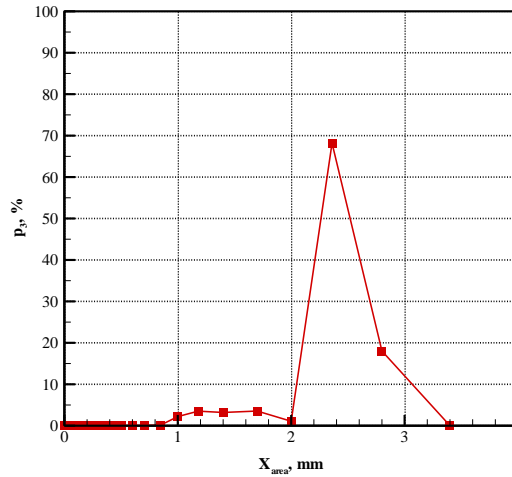
Figure 18. Statistical measurement of X_{area}

3.3. Thermogravimetric Analysis

As the properties of the irregularly shaped samples collected from the Avedøre power plant are unknown, a thermogravimetric analysis is conducted to compare the conversion behaviour of these samples (compressed wood) with that of the pine wood (uncompressed wood), whose properties are known. The pine wood is chopped into small flakes with sizes similar to those of the milled particles. The tests are performed at 5% oxygen concentration and three different heating rates: 5, 50 and 500 K/min. Figure 19 and Figure 20 show the TG set-up located in the laboratory of the CHEC group at the Technical University of Denmark and the samples studied, respectively.
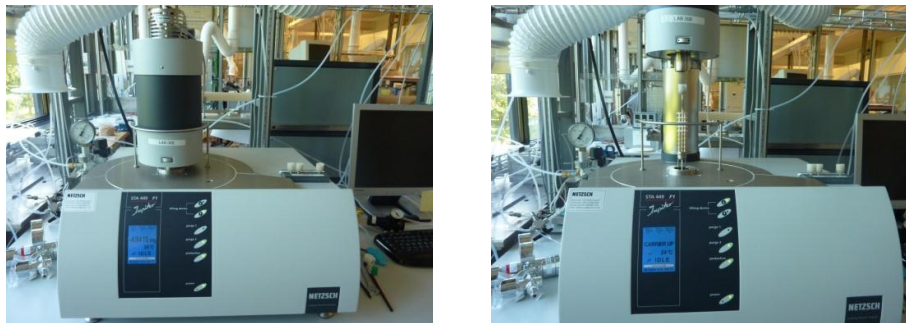
Figure 19. TG set-up
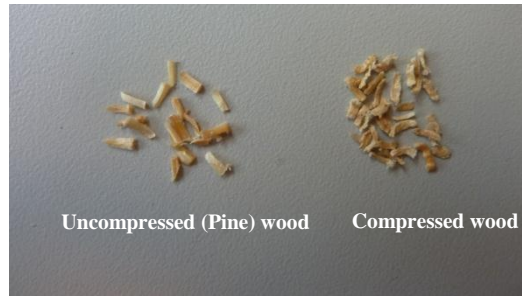
Figure 20. Compressed and uncompressed samples for TG analysis

The results show that the two types of samples have similar conversion behaviours across a range of different conditions (heating rates). Figure 21and Figure 22 illustrate the mass loss of the samples versus temperature and time. Based on these results, due to the lack of information about the properties of the irregularly shaped particles, the properties of pine wood (from the ultimate and proximate analyses) are used for modelling.
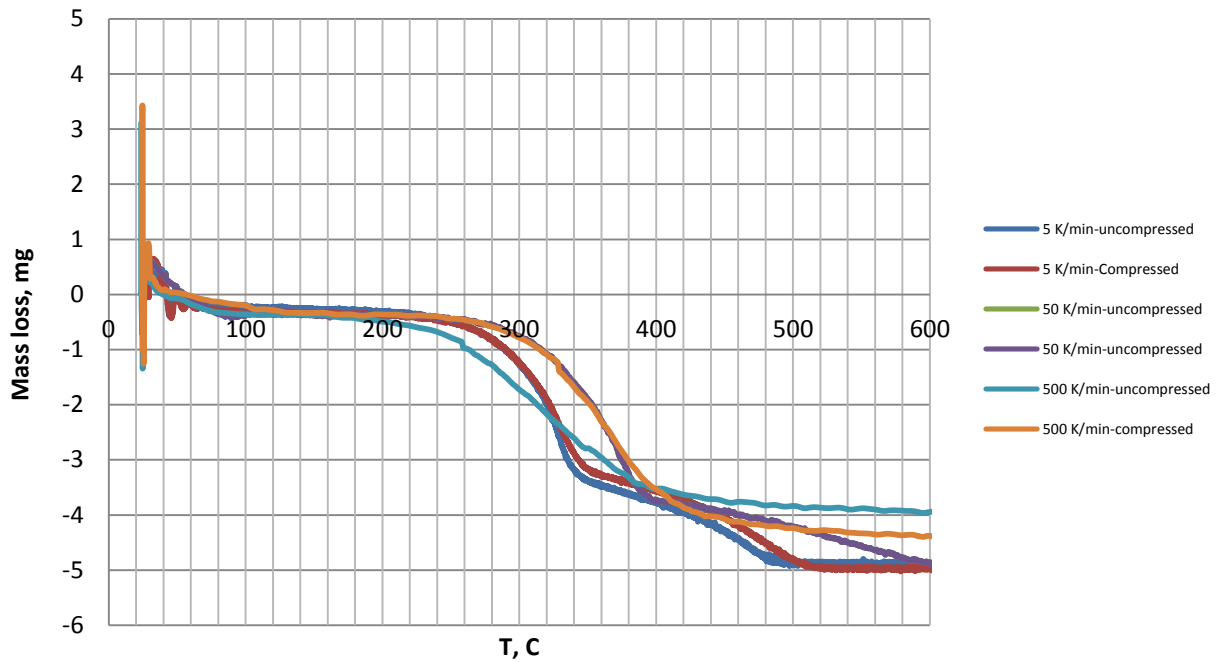
Figure 21. Mass loss vs. temperature determined by TG analysis at 5% O_2

Figure 22. Mass loss vs. time determined by TG analysis at 5% O_2

3.4. Experimental procedure

The temperature and oxygen profiles inside the reactor are measured by inserting a suction pyrometer and a suction probe into the reactor at the desired location between the wall and the reactor centre. The measurements are conducted at both the left and right sides of the reactor. Due to the burner design, gas flow containing oxygen has more space at the outer radius inside the reactor, which, together with the heat loss to the surroundin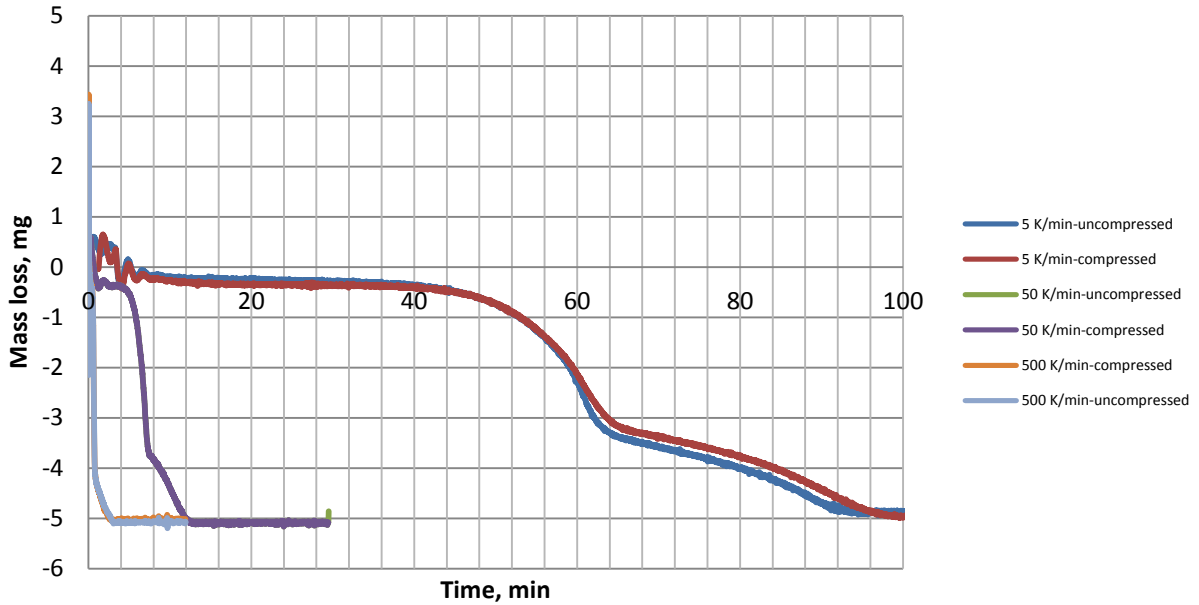gs, induces colder flow in the near-sidewall zones than in the reactor center. As an example of the measurements, Figure 23 shows the temperature and oxygen concentration profiles for values of the inlet flows such that the fuel particle is exposed to a temperature of 1400°C and an oxygen concentration of 5 vol% in the centre of reactor. The centre-line condition is assumed to be representative of a fuel particle experiment as the particle diameter is less than 6% of reactor diameter.

The biomass particles ignite very quickly, such that a particle can ignite immediately following insertion even before reaching the reactor centre. Consequently, a ceramic protection tube is used to shield the particle and allow the particle to reach the centre before ignition. The tube is made of a non-porous ceramic (Al_2O_3) with a thermal conductivity of 30 W/mK. Figure 24 shows the protection tube and its location in the reactor.

31
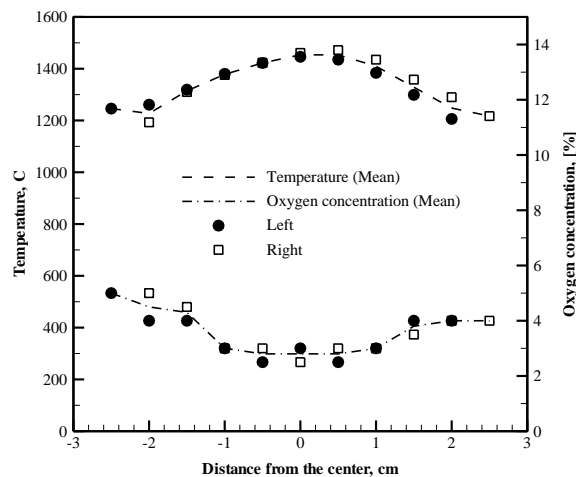
Figure 23. Temperature and oxygen concentration profiles (T_{centre}=1400°C, $O_{2,centre}$=5%)

Figure 24. Protection tube and its location in the reactor

The protection tube is first inserted into the reactor, and then the particle is inserted on the platinum holder into the reactor through the protection tube from the opposing hole; the protection tube is then ejected from the reactor tube. All these steps occur very quickly (< 5 s) so that the heat transfer from the tube to the particle is negligible. Figure 25 shows the change in temperature with time for a thermocouple placed inside the protection tube or in the reactor after the protection tube is removed. The temperature is evidently very low for up to 10 s, demonstrating that the particle begins to be heated only when the protection tube is removed. When the protection tube is withdrawn, the particle is exposed to the hot gas, and the experiment is initiated.

Figure 25. Temperature variation vs. time inside the protection tube and the reactor

Figure 26 shows how the protection tube is removed to subject the particle to the hot flow; the speed of the procedure is also indicated (~ 0.03 s). No significantly slower or faster burning rates are observed near the platinum wire, and the size of the hole is always less than 10% of the particle size. The particle conversion process is monitored by a video camera. The flow is perpendicular to the main axis (length direction) of the particle.
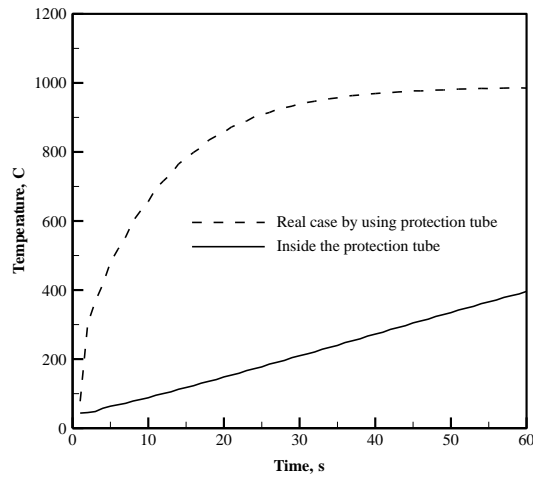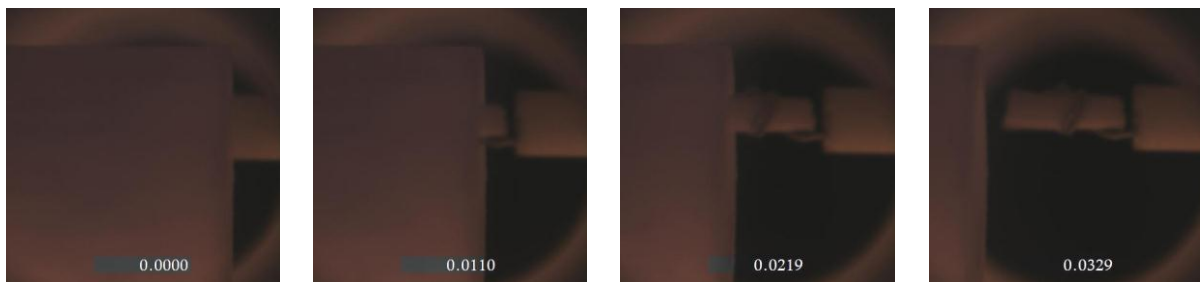

Figure 26. Removing the protection tube from the reactor

Operating conditions of high temperatures and high heating rates are used to produce conditions that are reasonably close to those in actual PF combustion. The temperature in the experiments varies over the 1200 to 1600°C range, and the oxygen concentration varies from 5 to 20%. Selected tests are repeated 3 to 5 times to ensure the characteristics and reproducibility of the results. Three different characteristic times can be determined from the collected videos: the ignition time, the total devolatilisation time and the burnout time. The criteria for determining the ignition, devolatilisation and burnout times are based on observations of images captured during the entire combustion process. The initial time (t_0) is always considered to be the time of the removal of the protection tube. The ignition time is assumed to correspond to the observation of the first flame in the images. After ignition, the visible devolatilisation process begins, during which period the flame around the particle is clearly apparent. When the flame disappears, the devolatilisation is assumed to have ceased, and the time recorded is considered to be the devolatilisation process time. The remaining char is then combusted without an apparent flame, and the char burning continues until

complete burnout. No change is observed in the particle (no shrinking/swelling). As the char burning process may overlap with the devolatilisation process, the char burnout time determined from the images is an underestimate of the actual char burnout time. Thus, in this study, the total time from the insertion of the particle into the reactor until the end of the combustion process is referred to as the burnout time. An example is illustrated in Figure 27, which shows how the three conversion times are estimated from the images taken of a cylindrical particle; from these images, 0.0549 s, 3.08 s and 8.22 s are determined as the ignition time, the devolatilisation time and the burnout time, respectively. For instance, the devolatilisation stage in Figure 27 clearly shows that the flame vanishes at 3.09 s, and the previous time step (3.08 s) is considered to be the end of the devolatilisation process.
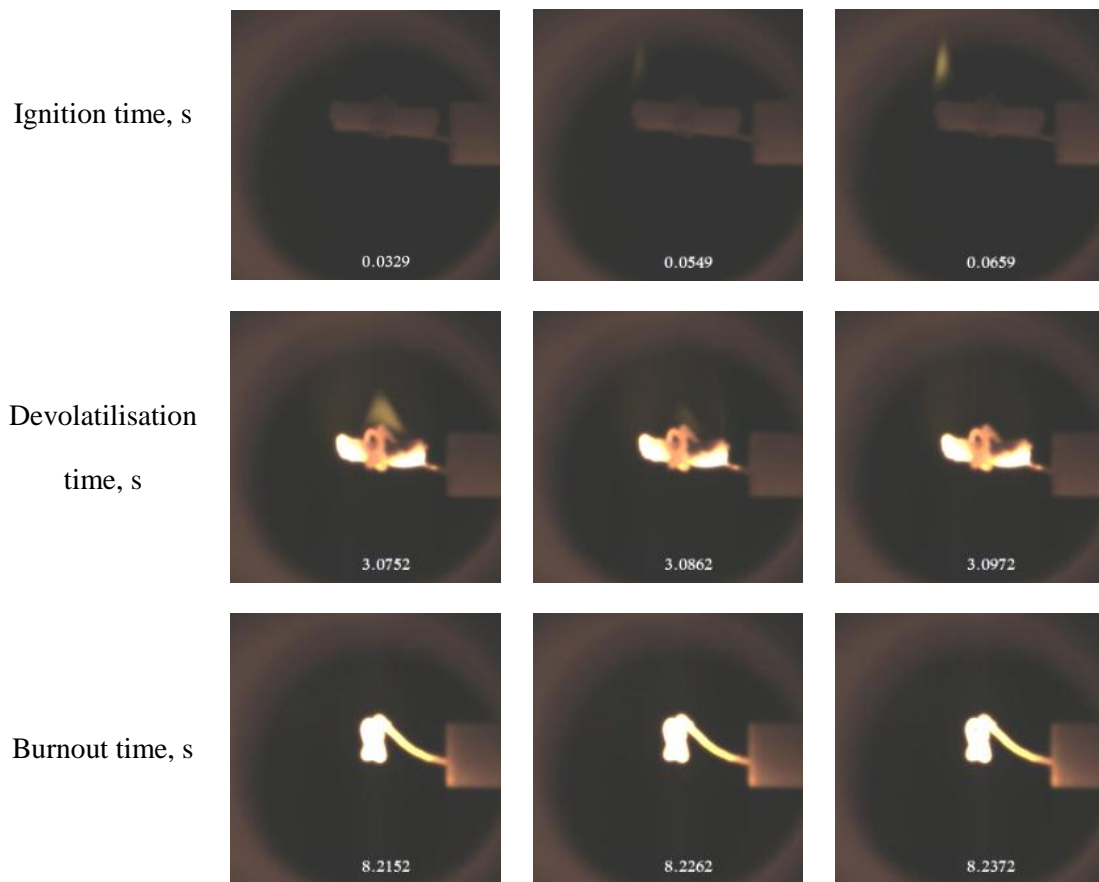

Figure 27. Selected images of a spherical particle at different stages of combustion

4

MODELING APPROACH

Modeling approach describes the mathematical model in details. Different steps of the particle combustion process are explained and all the governing equations are presented. The criteria applied for predicting different stages of particle combustion are discussed and implementation of particles information in the model are explained as well.

For a cold biomass particle suddenly exposed to a hot environment, it will be heated up and then undergo a series of conversion processes (e.g., drying, devolatilization, char gasification and oxidation). If all the parameters at time t are known, mathematical modelling of the conversion of a large, thermally-thick biomass particle for these parameters at a new time $t + \Delta t$ can be subdivided into three coupled issues: 1) heat and mass transfer to or away from the particle, 2) biomass particle conversion analysis, in which all the key intraparticle processes need to be appropriately considered for a thermally-thick particle, and 3) particle dynamics. The first issue only involves empirical correlations, the second is to solve some coupled partial differential equations, and the third needs to address a few ordinary differential equations.

The modlling study is based on the model developed by Lu et al. 2008. A sensitivity analysis was conducted to study the role of different sub-models and reduce the computational time.

4.1. Governing equations and boundary/initial conditions

In this study, particle dynamics issue is left out since the particle is suspended in the reactor without any movement. The intraparticle conversion analysis is the most challenging issue, in which the following governing equations are solved by using finite volume method to update the velocity, temperature and gas species profile in a porous biomass particle.

$$
\begin{cases}
\dfrac{\partial(\varepsilon\rho_g)}{\partial t} + div(\varepsilon\rho_g\vec{u}) = S_g \\[2mm]
\vec{u} = -\dfrac{\eta}{\mu}\dfrac{\partial p}{\partial r} \\[2mm]
\dfrac{\partial}{\partial t}\left(\sum_{\text{solid}i}\rho_i h_i + \sum_{\text{liquid}k}\rho_k h_k + \varepsilon\rho_g h \right) + div(\varepsilon\rho_g\vec{u}h) = div(k_{eff}\nabla T) + div(-\sum_j h_j\vec{J_j}) + S_h \\[2mm]
\dfrac{\partial}{\partial t}\left(\varepsilon\rho_g Y_j\right) + div(\varepsilon\rho_g\vec{u}Y_j) = div(-\vec{J_i}) + S_{Y_j}
\end{cases} \tag{2}
$$

where ε, ρ_g, t, $\vec{u}$, S_g, η, μ, p, r, h, k_{eff}, T, $\vec{J_j}$, S_h, Y_j and S_{Y_j} represent porosity, gas density, time, gas velocity, source term to gas mass conservation, permeability, gas dynamic viscosity, pressure, radius, sensible enthalpy, effective heat conductivity, temperature, diffusion flux of gas species j in the gas mixture, source term to the energy equation, mass fraction of gas species j, and source term to j-th gas species, respectively.

Here, it has to be mentioned that a simplified momentum equation (i.e., a Darcy law type equation) is used instead to evaluate gas velocity inside the porous particle. In the Darcy equation, the pressure is calculated from the ideal gas law, $p = \dfrac{\rho_g R_u T}{MW}$, in which R_u and MW denote the universal gas constant and molecular weight of local gas mixture, respectively. A local thermal equilibrium is assumed among the different phases inside the particle so that a lumped energy equation for all the phases is employed. In the energy equation, The sensible enthalpy of the gas mixture is calculated by $h = \sum_j Y_j h_j$, where the sensible enthalpy of individual gas species is defined as $h_j = \int_{T_{ref}}^{T} C_{p,j}(T)dT$. The diffusion flux of gas species j in the gas mixture is evaluated by $\vec{J_i} = -\rho_g D_{j,m}\nabla Y_j$, where $D_{j,m}$ is the effective mass diffusivity of species j in the gas mixture. Here, the general governing equations, rather than particle shape or problem dimension-dependent equations, are employed. The former can be better and more conveniently integrated into finite volume method than the latter, provided the physical meaning of the governing equations and finite volume method and the basic knowledge in calculating distance, surface area and cell volume under various coordinate systems.

Here, all the parameters (e.g., velocity, temperature and species) are assumed to vary only in the radial direction. So it turns out to be a transient, 1D problem, in which the governing equations are solved under the following free-stream (or process) condition, initial condition and boundary conditions (BCs):

$$\begin{cases} \text{Free-stream condition}: \ T_\infty = T_f, u_\infty = U_f, Y_{O_2,\infty} = 0.23, Y_{N_2,\infty} = 0.77, \rho_\infty = \rho_f \\[4pt] \text{Initial condition in particle}: \ u = 0, \ p = p_{\text{atm}}, \ T = 300K, \ Y_j = 0 \\[4pt] \text{BCs at particle center}: \ \left.\dfrac{\partial \phi}{\partial r}\right|_{r=0} = 0 \quad (\text{symmetry}) \\[8pt] \text{BCs at particle surface}: \ p\big|_s = p_{\text{atm}} \\[6pt] \qquad\qquad k_{eff} A_s \left.\dfrac{\partial T}{\partial r}\right|_s = h_T A_s (T_\infty - T_s) + \varepsilon_{emis}\sigma A_s (T_{rad}^4 - T_s^4) \\[8pt] \qquad\qquad D_{j,m} A_s \left.\dfrac{\partial Y_j}{\partial r}\right|_s = h_M A_s (Y_{j,\infty} - Y_{j,s}) \end{cases} \tag{3}$$

where the subscripts, ∞ and s, denote the free-stream and the particle surface, respectively. A_s, ε_{emis}, σ, h_T, T_{rad} and h_M are particle surface area, emissivity, Stefan-Boltzman constant, heat transfer coefficient, radiation temperature, and mass transfer coefficient, respectively.

To reliably handle the boundary conditions at the particle surface, empirical correlations that are applicable to a certain particle shape and appropriately account for the Stefan flow effect need to be used to calculate the convective heat and mass transfer coefficients, h_T and h_M. The resistance to the convective heat and mass exchange between the particle surface and the free-stream gas flow is assumed to be within a gas film (or boundary layer) of constant thickness, δ_T, δ_M. For instance, for spherical particles without Stefan flow effect, the heat and mass transfer coefficients can be calculated as follows,

$$\begin{cases} Nu_0 \equiv \dfrac{h_T d_p}{\overline{k_g}} = 2.0 + 0.64\,\text{Re}^{0.5}\,\overline{\text{Pr}}^{0.33} \\[10pt] Sh_0 \equiv \dfrac{h_M d_p}{\overline{D_g}} = 2.0 + 0.64\,\text{Re}^{0.5}\,\overline{\text{Sc}}^{0.33} \end{cases} \tag{4}$$

where Nu_0, Sh_0, and d_p represent Nusselt number, Sherwood number and particle diameter, respectively. The average physical properties in the gas film need to be used in Eq. (3). For example, the average gas conductivity $\overline{k_g}$, gas diffusion coefficient $\overline{D_g}$, viscosity $\overline{\mu_g}$, Prandtl number $\overline{\text{Pr}}$, and Schmidt number $\overline{\text{Sc}}$ are all evaluated at some reference temperature and gas species mass fraction, e.g.,

$$T_{ref} = T_s + \tfrac{1}{3}(T_\infty - T_s); \qquad Y_{j,ref} = Y_{j,s} + \tfrac{1}{3}(Y_{j,\infty} - Y_{j,s}) \tag{5}$$

The Reynolds number in Eq. (3) is calculated based on the free-stream density ρ_∞ and the average viscosity $\overline{\mu_g}$ in the gas film, $\text{Re} = \dfrac{\rho_\infty |u_\infty - u_p| d_p}{\overline{\mu_g}}$, since it is interpreted as a ratio of

inertia to viscous forces. The thickness of the gas film for heat and mass transfer without Stefan flow effect, δ_{T0} and δ_{M0}, can be calculated as follows,

$$\delta_{T0} = \frac{d_p}{Nu_0 - 2}; \qquad \delta_{M0} = \frac{d_p}{Sh_0 - 2} \tag{6}$$

In this study, the effect of the Stefan flow is accounted in the calculation of the heat and mass transfer coefficients. A surface blowing results in the thickening of the heat and mass transfer boundary layer by a factor of F_T and F_M, respectively,

$$\begin{cases} F_T \equiv \dfrac{\delta_T}{\delta_{T0}} = (1 + B_T)^{0.7} \dfrac{\ln(1 + B_T)}{B_T} \\[2mm] F_M \equiv \dfrac{\delta_M}{\delta_{M0}} = (1 + B_M)^{0.7} \dfrac{\ln(1 + B_M)}{B_M} \end{cases} \tag{7}$$

where B_T and B_M represent the Spalding heat and mass transfer numbers, respectively. When the Stefan flow effect is taken into accounted, the Nusselt and Sherwood number can be calculated as follows,

$$\begin{cases} Nu = 2 + (Nu_0 - 2)/F_T \\ Sh = 2 + (Sh_0 - 2)/F_M \end{cases} \tag{8}$$

from which the heat and mass transfer coefficients, h_T and h_M, to be used in the boundary conditions can be evaluated. The boundary layer domain with thickness of δ_T and δ_M can be included in the modeling.

For other particle shapes, e.g., cylindrical particles, the similar process as above needs to be followed. The main difference is to replace Eq. (4) with different correlations that are applicable to other particle shapes.

4.2. Particle conversion sub-processes

In the governing equations, Eq. (2), the number of gas species transport equations and the various source terms depend on how the physical conversion processes are considered.

For the drying processing, the release of both the free water and bound water can be taken into account, as shown in Table 7 which summarizes not only all reactions involved but also their rate expressions and kinetic data. Moisture content above fiber saturation point (FSP) is assumed as free water and exists in pores and cells in liquid form. Moisture content below the FSP is considered as bound water, which exists as hydrate species in the particle. The average FSP is about 30% and the moisture content of the wood particle samples used in this study is about 10%. Therefore, all the moisture has been presumed as bound water in modelling and it

is released by chemical reaction [Forest Products Laboratory United States Department of Agriculture Forest Service, 1999].

When the particle is further heated up, biomass starts to be decomposed to non-condensable gases, condensable species (e.g., water and organic compounds) and char via different reaction routines, in which the organic vapor degrade further to form chars, non-condensable gases and water if held in contact with the solid biomass undergoing devolatilization, as sketched in [Yin et al. 2012]. Accordingly, a two-step devolatilization model is used in this work. The biomass is decomposed to light gases, tar and char. Then, the tar can be further converted into light gases and char, as shown in Table 7, in which the composition of the light gases and the three homogeneous reactions are also given.

The char left in biomass particle can be oxidized via various ways, depending on the gas species available in the solid matrix and at the particle surface. Here, three heterogeneous reactions are considered: char oxidation with oxygen, carbon dioxide and water vapour, respectively, as shown in Table 7.

From Table 7, the density of various solid and liquid species can be easily updated from the ordinary differential equations. The source terms in the continuity equation, energy equation and various species transport equations can also be readily evaluated.

Table 7. Chemical reactions considered: the rate expressions and kinetic data used in $k = AT^b e^{-E/(R_u T)}$

Sub-process	Reactions	Rate expressions	A [1/s]	b	E [kJ/mol]	ΔH [kJ/kg]
Evaporation	H_2O(l, free)↔H_2O(g)	$r_1 = \dfrac{\partial \rho_{fw}}{\partial t} = S_a \dfrac{\rho_{fw}}{\rho_{fw}^0} h_{m,pore}(\rho_v^{sat} - Y_v \rho_g)$				-2440
	H_2O(l, bound)→H_2O(g)	$r_2 = \dfrac{\partial \rho_{bw}}{\partial t} = k_2 \rho_{bw}$	5.13e+10	0	88	
Devolatilization	Biomass → light gas *	$r_3 = \dfrac{\partial \rho_B}{\partial t} = k_3 \rho_B$	4.38e+9	0	152.7	
	Biomass → tar	$r_4 = \dfrac{\partial \rho_B}{\partial t} = k_4 \rho_B$	1.08e+10	0	148	-418
	Biomass → char	$r_5 = \dfrac{\partial \rho_B}{\partial t} = k_5 \rho_B$	3.27e+6	0	111.7	
	Tar → light gas	$r_6 = \dfrac{\partial \rho_G}{\partial t} = \varepsilon k_6 \rho_g Y_T$	4.28e+6	0	107.5	42
	Tar → char	$r_7 = \dfrac{\partial \rho_C}{\partial t} = \varepsilon k_7 \rho_g Y_T$	1.0e+5	0	107.5	
Light gas combustion	$CO+O_2 \rightarrow CO_2$	$r_8 = \dfrac{\partial [CO]}{\partial t} = k_8 [CO][O_2]^{0.25}[H_2O]^{0.5}$	1e+12.35	0	167	10110
	$H_2+O_2 \rightarrow H_2O$	$r_9 = \dfrac{\partial [H_2]}{\partial t} = k_9 [H_2][O_2]^{1.42}$	1e+12.71	0	171.3	120900
	$C_xH_yO_z+O_2 \rightarrow CO+H_2$	$r_{10} = \dfrac{\partial [HC]}{\partial t} = k_{10}[HC]^{0.5}[O_2]$	1e+4.32·T·P^0.3	0	80.2	41600
Char oxidation	$C+O_2 \rightarrow CO$	$r_{11} = \dfrac{\partial [O_2]}{\partial t} = \dfrac{S_{a,char}\rho_C}{\rho_C+\rho_B+\rho_A} \varepsilon k_{11}[O_2]$	0.658 m/(s·K)	1	74.8	9212
	$C+CO_2 \rightarrow CO$	$r_{12} = \dfrac{\partial [CO_2]}{\partial t} = \dfrac{S_{a,char}\rho_C}{\rho_C+\rho_B+\rho_A} \varepsilon k_{12}[CO_2]$	3.42 m/(s·K)	1	130	14370
	$C+H_2O \rightarrow CO+H_2$	$r_{13} = \dfrac{\partial [H_2O]}{\partial t} = \dfrac{S_{a,char}\rho_C}{\rho_C+\rho_B+\rho_A} \varepsilon k_{13}[H_2O]$	3.42 m/(s·K)	1	130	10940

*: The composition of the light gas produced during devolatilization process: CO=0.396, CO_2=0.209, H_2=0.019, H_2O=0.249, light hydrocarbon ($C_6H_{6.2}O_{0.2}$)=0.127 in mass fraction. Unit of [Gas]: kg gas per m^3. The 1st step devolatilization: kinetic data from [Di Blasi and Branca 2001] and heat of reaction from [Chan et al. 1985]. The 2nd step devolatilization: kinetic data for Tar → light gas from [Liden et al. 1988]; kinetic data for Tar →char from [Di Blasi 1993]; heat of both the reactions from [Koufopanos et al. 1991].

4.3. Physical properties

After the detailed particle conversion mechanism is addressed, as summarized in Table 7, the remaining issue to close the system of equations and make it solvable is to evaluate physical properties of the raw biomass particles, as well as all the solid, liquid and gas species involved in the conversion mechanism. The approximate and ultimate analysis, heating value and density of the pine wood are given in Chapter 3. Other data about the pine wood particles, e.g., porosity ε, emissivity ε_{emis}, permeability η, pore size d_{pore}, heat conductivity k, specific heat C_p, biomass particle specific surface area S_a, char particle specific surface area $S_{a,char}$, are taken from [Lu et al. 2008]. All the physical properties of

water and various gas species considered in the model are readily available in handbooks, e.g., [Perry's Chemical Engineers' Handbook]

4.4. Numerical method

The particle is divided into a number of spherical shells (or cells) in radial direction. The governing partial differential equations in Eq. (2) are discretized using the finite volume method. For all the transport equations, the fully implicit scheme is used for the transient terms and the power law scheme is employed for the convective-diffusion terms, both of which are readily implemented. Since quite some reactions which are highly non-linear are considered in the conversion mechanism, the source terms in the continuity, energy and various species transport equations are cumbersome. Appropriate treatment of the source terms is crucial to assure the stability of such a single particle model, as discussed in [Yin et al. 2010]. The source terms are linearized by following the rule of negative-slope linearization [Patankar 1980], as demonstrated in discretizing the energy equation on the outermost cell in a simplified single particle model [Yin et al. 2010].

Such a model has been validated against experiments in terms of the temperatures at centre and surface of various particles (e.g., near-spherical or cylindrical) and the mass loss under different conditions, e.g., during pyrolysis in nitrogen [Lu et al. 2008]. Here, the focus of the modelling is to extend the study to the ignition, devolatilization and char oxidation of various biomass particles under process conditions that are similar to those in an industrial combustor and compare the model prediction with our experimental results.

Results and Discussions

The main results of the current project are summarised, including the experimental results, the modelling results and the validation. The results are divided to two groups: particles with regular shapes and particles with irregular shapes. The results that are summarised in this section are discussed comprehensively in the written papers attached to the end of the thesis.

In this project, biomass particle combustion experiments are conducted in a single particle reactor. For the single particle reactor, combustion data for wood particles, including ignition, devolatilisation and burnout, are collected in the form of video sequences under different conditions.

All the data are compared with the predictions of the one-dimensional single particle combustion model described in chapter 4.

In this chapter, the single particle combustion model is validated using data for the particle conversion times collected from the single particle reactor. Additionally, the effects of the particle shape, operating conditions (oxygen concentrations and oxidiser temperatures) and the milling process on different stages of particle conversion (ignition, devolatilisation and burnout) are thoroughly discussed.

The samples used in this study are categorised in two groups:

- o Regularly shaped particles

  - Wood (pine wood) particles of identical volumes and spherical shapes with diameters of 3 mm and cylinders with varying aspect ratios (AR=length/diameter =2, 4, 6 and 8);
  - Three different cylindrical particles with similar diameters (3 mm) but with different lengths and, consequently, different volumes;

o Irregularly shaped particles

Single pulverised particles with irregular shapes were collected from the Avedøre power plant from two different milling processes:

- Particles from hammer mill trials
- Particles from roller mill

All the physical and chemical properties of the samples are presented in chapter 3; the estimation of the particle shapes using information obtained from the CAMSIZER and the use of the shape data in the 1D model were discussed in detail in chapter 4.

5.1. Effects of particle shape and size

As it was discussed before pulverized biomass particles depend on mill used are typically larger than coal particles.
Abbas et al. 1996, found that the grinding of biomass consumes energy almost two times more than the required energy for coal. So, such a huge cost causes to tend cofiring large biomass particles (> 1mm) which have economical advantages. From the other side, the larger particles raise additional concerns about boiler operability due to the unburned carbon. Biomass also has higher volatiles contents compared to coal. So a large amount of biomass is converted to the gaseous products through the devolatilization process at temperature lower than combustion temperature. From the technical point of view, it is important to be able to understand devolatilization process and its role in the combustion of a single particle and also find out how fast it takes place for a single particle with diameter of a few millimeters under the real operating conditions.
Thus, estimating the conversion time of particles with different shapes and sizes has essential role in designing utility boilers with appropriate residence time to minimize unburnt carbon of large biomass particles and optimization purposes. On the other hand, this kind of study also helps to have correct approximation of particles in terms of modelling.
In this study, the first group of samples, the regularly shaped particles, are used to study the effects of shape and size on particle conversion.
The conversion time for particles of different shapes and sizes at a fixed temperature of 1200 °C and a 21% oxygen concentration are discussed in this section.

Ignition

A study on fuel particle ignition often involves ignition delay, ignition temperature and ignition mechanism, and their dependency on fuel properties and process conditions.
Ignition indicators that are commonly used in experimental studies include, e.g., detection of a light flash, increase in the luminous flux, change in the mass loss, increase in particle temperature, rapid decrease in CO and O_2 combined with increase in CO_2 and NO, increase

in CO_2/CO ratio, exothermic peaks on differential thermal analysis curves combined with mass loss, devolatilization images [Essenhigh et al. 1989, Zhang and Wall 1994, Chen et al. 1996, Grotkjær et al. 2003, Faúndez et al. 2005, Kuo and Hsi 2005, Shaddix and Molina 2009]. Ignition indicators may have a significant impact on the estimated ignition delay, ignition temperature or even ignition mechanism. In the current experimental study, a light flash is used as the ignition indicator, since neither the particle temperature/mass nor the evolved gases are measured. From the light flash, it is very hard to distinguish the ignition mechanism in such an experimental condition in which both the upward gas velocity (~1.5m/s) and gravity-induced buoyancy play important roles in the shape and position of the flame. It is even impossible to distinguish whether the flash is due to volatile matter ignition or char ignition. As an example, Figure 28 shows the ignition process of a spherical pine wood particle (3mm in diameter) in the reactor with ambient air temperature of 1200 °C, molar fraction of oxygen of 21%, and superficial air velocity of 1.5 m/s. From the images, one may conclude that the ignition delay is 0.1318s, i.e., the first image corresponds to the onset of ignition.

Figure 28. Ignition of a spherical particle (d_p=3mm) in the reactor (T=1200°C and O_2=21%).

To clarify the ignition mechanisms, simulations are done using the somehow validated model, from which much more detailed information can be extracted, e.g., the instantaneous temperature and species profiles inside the particle and in the boundary layer surrounding the particle, reaction rates and mass loss of the particle. The ignition mechanisms and the possible shift between them can be located, once quantitative ignition criteria are available. Different criteria were applied to predict ignition moment, temperature and ignition mode. The experimental and modelling results were discussed in detail in Paper 1 and 2.

For homogeneous ignition, both the experimental and modeling results show the similar trend as theoretical expectation, i.e., the larger the specific surface area is, the shorter the homogeneous ignition delays will be. However, the heterogeneous ignition delays may not precisely scale with the specific surfaces, which is consistent with the findings of [Wendt et al. 2002]. The effect of shape on particle ignition may not be explained simply in terms of specific surface areas since ignition depends on complex interactions involving external and internal heat and mass transfer and chemical reactions.

Devolatilisation and Burnout

Devolatilization and burnout characteristics of small single biomass particles (3.0 mm) and the effects of particle shape on the particle conversion time have been investigated. The

results provide a database of single particle devolatilization and burnout time with relevant size and different shapes.

The estimation of particle devolatilisation and burnout times from the experimental data and by the model are explained in chapters 3 and 4, respectively.

Figure 29 and Figure 30 show how devolatilisation, char burning and burnout times change with the particle shape, based on both numerical predictions and experimental results. The results show that among samples with similar volumes (or masses), spherical particles have longer devolatilisation and burnout times compared to cylindrical particles. This is because a spherical particle has a lower surface area to volume ratio than a cylindrical particle of the same volume (mass). Therefore, particles with a higher aspect ratio will heat up more rapidly by external convection and radiation due to their larger external surface area, which results in a faster conversion rate. So it indicates that equivalent sphere is a poor approximation in modelling and predicting the conversion time of particles.

This same study is performed for the irregularly shaped particles in different size classes: d=2 mm and 3 mm. The results show that particles with different dimensions have similar conversion times when their surface area to volume ratios are equal. More details on these results can be found in papers 1 to 3.
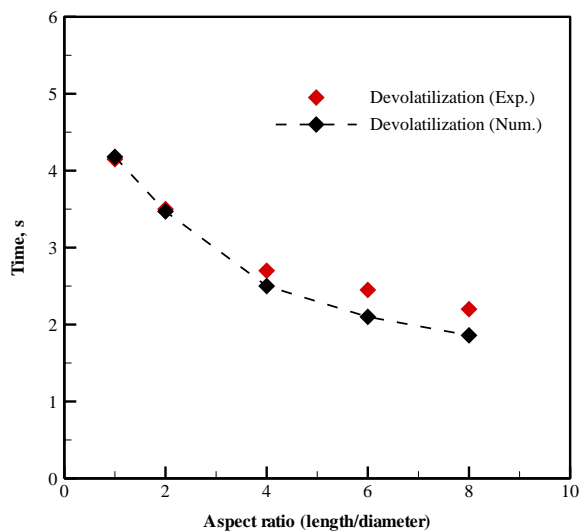

Figure 29. Devolatilisation time vs. particle aspect ratio at T=1200°C and O_2=21% (an aspect ratio of 1 corresponds to a spherical particle)

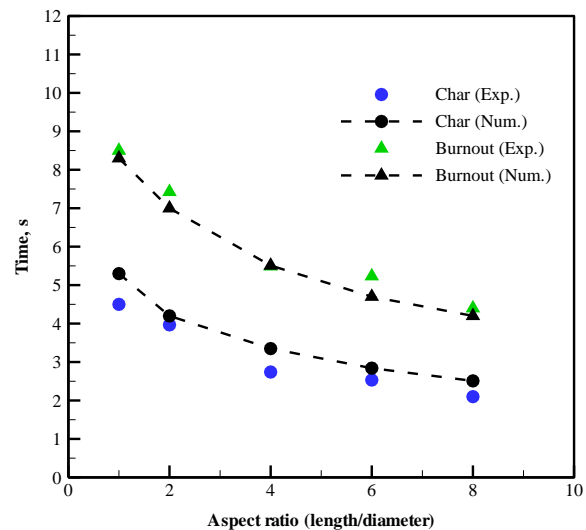**Figure 30.** Char burning and burnout times vs. particle aspect ratio at T=1200°C and O_2=21% (an aspect ratio of 1 corresponds to a spherical particle)

5.2. Effects of operating conditions

The conversion characteristics of the irregularly shaped pulverised particles (d=3.0 mm) from the Avedøre power plant, is investigated under different surrounding conditions. The temperatures vary from 1200°C to 1600°C, and the oxygen concentrations are in the 5-20% range.

As previously explained, the sizes and shapes of the pulverised particles are analysed using a CAMSIZER, and the particle volumes are calculated from the measured densities and masses of individual particles. All the physical and chemical properties of the two groups of samples can be found in chapter 3; the estimation of the particle shape from the CAMSIZER and the use of the particle shape in the 1D model are detailed in chapter 4.

Figure 31 illustrate the effects of the oxidiser temperature and the oxygen concentration on the particle devolatilisation times for a regularly shaped cylindrical particle with an aspect ratio of 4 and an irregularly shaped pulverised particle with a diameter of ~3 mm, respectively.

As previously explained, the devolatilisation time is defined in this study as the time interval between inserting the particle into the reactor and the moment of combustion of all the volatiles. Increasing the oxygen concentration speeds up the homogeneous combustion of the released volatiles, which, in turn, intensifies the local heat release. Therefore, higher oxygen concentrations are expected to shorten the devolatilisation time, as shown in Figure 31. For large particle sizes and high particle temperatures, the diffusion resistance is the limiting factor, while the kinetic resistance dominates for small particle sizes and low particle temperatures. Thus, increasing the oxygen concentration of the bulk flow will always dramatically speed up the char oxidation process, exactly as observed in the experimental and numerical results in Figure 32. At comparatively low temperatures (e.g., T=1200°C), the kinetic resistance plays an important role in the process. In such a situation, an increase in the oxygen concentration may have two effects. The char oxidation is intensified and the volatile combustion is enhanced, which, in turn, intensifies the heat release around the particle and dramatically increases the particle temperatures such that the kinetic resistance becomes negligible. Thus, the effect of increasing the oxygen concentration is expected to be more pronounced at low temperatures than at high temperatures. At high temperatures, the kinetic resistance is always negligible. This expectation is also confirmed by both the experimental and numerical studies, as shown in Figure 32.
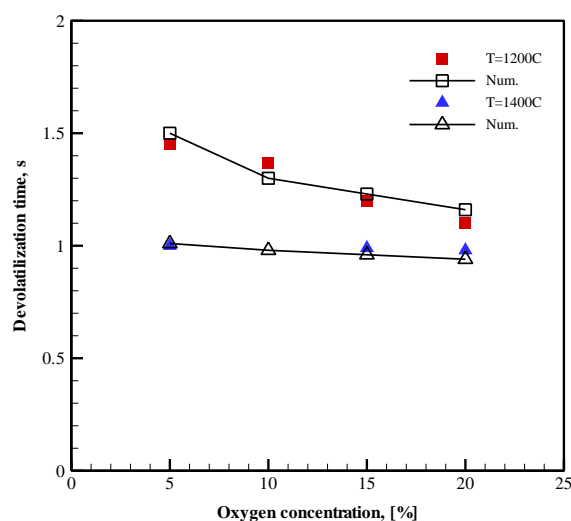

Figure 31. Devolatilisation time vs. oxygen concentration for a pulverised particle at different temperatures (d=3.0 mm)
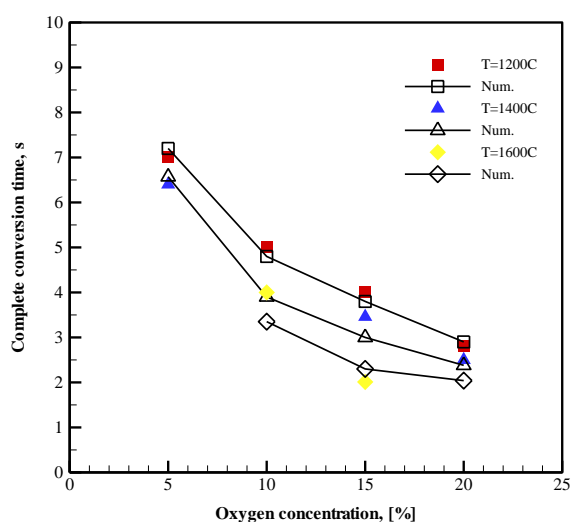
Figure 32. Time for complete conversion vs. oxygen concentration for a pulverised particle at different temperatures (d=3.0 mm)

The effects of operating conditions on the conversion of both regularly shaped and irregularly shaped particles are discussed in detail in the attached papers.

5.3. Effects of the milling process

As shown in chapter 3, comminuted wood pellet particles are collected from two separate sources:

- DONG Energy hammer mill trials at Sdr. Stenderup, 18-19 February 2011 (sample # 3.100KOL-8)

- Roller-milled wood pellet samples from a transport pipe to burner 31 at AVV2, 7 January 2011 (sample #1658-10)

A portion (~100 g) of the two groups of samples is sieved, and the portion that is retained on a 2.8 mm mesh is collected for shape and size analysis by the CAMSIZER. Figure 33 and Figure 34 show the size and shape information obtained from the CAMSIZER analyser for the samples from two different milling processes.

Additionally, particles with similar structures are selected from each fraction and are weighed on an accurate balance before the combustion tests. The average mass (~8.93 mg) of the particles from the roller mill collected at AVV2 that are retained on the 2.8 mm mesh is larger than the average mass (~3.57 mg) of the particles from the hammer mill trials that are retained on a mesh of the same size. This result indicates that different particle sizes are produced by the different milling technique and that the roller-milled samples are much larger than the hammer-milled samples.
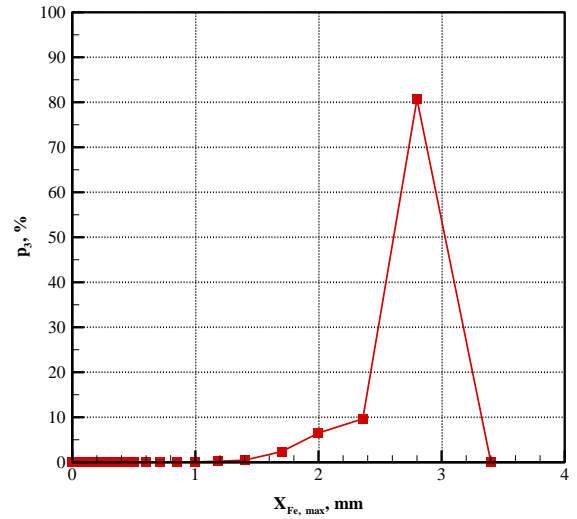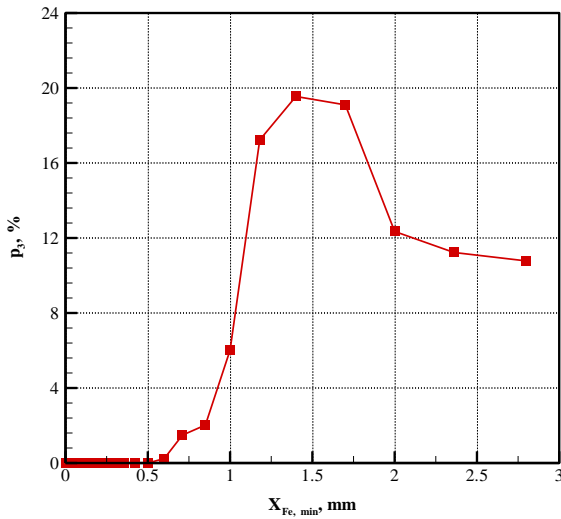
Figure 33. Statistics of particle dimensions (length and diameter) for 3.100KOL-8
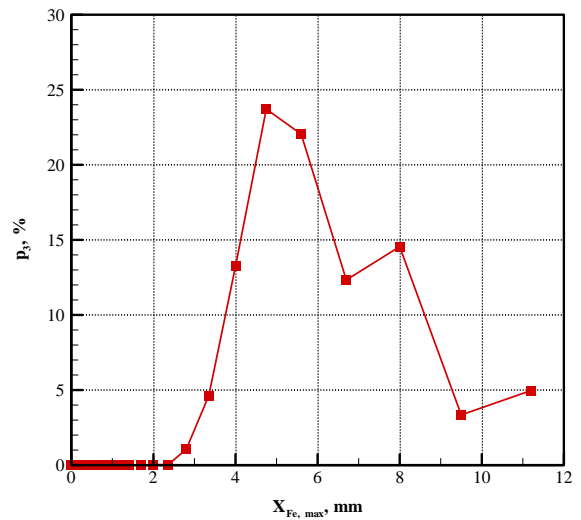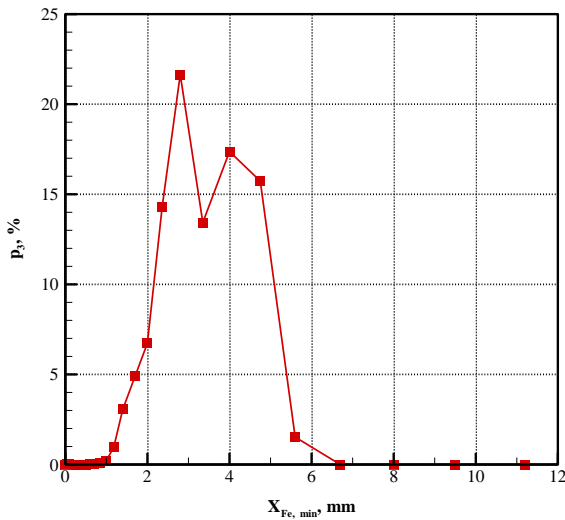

Figure 34. Statistics of particle dimensions (length and diameter) for 1658-10

Combustion tests are performed at 2 different temperature set-points (1400°C and 1600°C) and 4 different oxygen levels (5%, 10%, 15% and 20%) to compare and study the effects of the milling process on the particle conversion time. Different surface area to volume ratios are obtained for different particle sizes and masses. Consequently, the conversion times obtained from the combustion tests are normalised by the surface area to volume ratio from the CAMSIZER analysis and the measured mass and density for each particle. Figure 35 shows the normalised time for complete conversion for the two groups of samples at different oxygen concentrations and temperatures.

The results show that the two groups of samples from the different milling processes exhibit similar conversion behaviour regardless of their size distributions.

Figure 35. Particle conversion time normalised by the surface area to volume ratio vs. oxygen concentration at temperatures of 1400°C and 1600°C
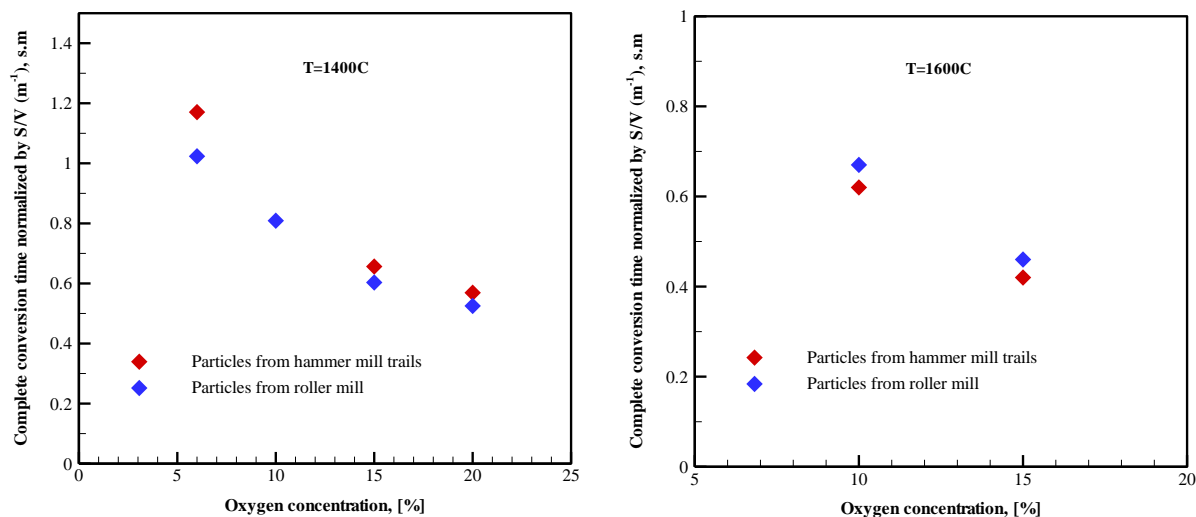
Summary- The ignition, devolatilization and burnout of biomass particles in a pf furnace (a few millimeters in diameter) were studied experimentally in a single particle combustion reactor rig, in which the ambient gas temperature and oxygen concentration can vary in the range of 1200-1600 °C and 5-20%, respectively. A 1D transient model is also used to predict their conversion, in which the key processes inside the particle and in the boundary layer outside the particle were properly considered.

For the particles in which large temperature gradients exist, the primary heterogeneous ignition is always detected for all the test conditions. As the particle is further heated up and the volume-weighted average temperature reaches the onset of rapid decomposition of hemicellulose and cellulose, a secondary homogeneous ignition occurs. The ignition, devolatilization and burnout are also affected by the process conditions, in which the oxygen concentration is found to have a more pronounced impact on the ignition delays, devolatilization and burnout times at lower oxidizer temperatures.

Different milling processes do not affect the conversion behaviour of particles regardless of their size distributions.

49

6

CONCLUSION AND FUTURE WORKS

The main conclusions of the current research project are highlighted, along with the improvement in the accuracy of the results contributed by this work. The possibilities for improving the work in the future are also addressed.

6.1. Accomplishments

In this PhD thesis, experimental data are collected, and a single particle combustion model is used to investigate the ignition, devolatilisation, and char burnout of single biomass particles of varying shape and size. Experimental data are collected in a single particle reactor. The particle dimensions and the surface areas of irregular particles are measured with a CAMSIZER analyser in this research project.

The accomplishments of each part of this project are as follows:

- A single particle reactor is used in this project to provide unique access to the combustion of single particles with different shapes under a variety of operating conditions. The set-up provides optical access to record the particle conversion processes. A maximum temperature of 1600 °C is used in the reactor. A high performance CCD camera is used to record the entire combustion process in the reactor.

- A CAMSIZER analyser is used to measure the particle dimensions and the external surface areas of the irregularly shaped particles.

- A single particle combustion model is used to simulate the combustion experiments. The model is able to simulate all the intraparticle conversion processes involved, including drying, recondensation, devolatilisation, char gasification/oxidation and swelling/shrinking, as well as the gas-phase combustion surrounding the biomass particles, for comparison with experimental data. Comparisons are made for particle conversion times at different stages. The model predictions provide a substantial

amount of additional data for biomass combustion that are difficult to measure directly.

- The particle shape and size impact fuel reactivity significantly. A comprehensive data set for biomass particle combustion is obtained as a function of the sample shape and size, the milling process and the surrounding conditions in the single particle reactor. The single particle combustion model provides a theoretical basis for analysing the experimental results.

6.2. Principal conclusions

- Both experimental and theoretical investigations indicate that the particle shape and size affect particle conversion significantly. Experiments conducted on biomass particles at commercially relevant temperatures for a variety of commercially relevant shapes and sizes show that the particle shape changes the overall conversion rates relative to particles of similar mass/volume by factors of two or more. The experimental data and theoretical models illustrate that the influence of the shape increases as the size and asphericity increase and that this influence is large at sizes relevant to industrial biomass utilisation. Generally, spherical mathematical approximations for particles that are aspherical during combustion poorly represent combustion behaviour at size scales relevant to industrial applications.

- In particular, the combustion of biomass particles on the scale of a few millimetres in a pulverized fuel boiler is a thermally thick regime. So intra-particle gradients strongly affect the predicted conversion time and particles react more slowly than predicted by lumped models (thermally thin). Such models underestimate volatiles release and combustion time which have a significant effects on boiler performance such as flame length, temperature profile, pollutant emissions, fouling, slagging and etc.

- Regarding operating conditions, increasing the gas temperature and oxygen concentration favours all of the sub-processes of biomass combustion, among which the effect of the oxygen concentration on char oxidation is more pronounced at comparatively low temperatures than at high temperatures.

- The data and model predictions in this study describe single biomass particle combustion rates reasonably well. Differences between the measurements and the predictions may be related to uncertainties in the physical properties, experimental procedure, or model assumptions in this approach.

6.3. Future works

From this study, several areas for future works are recommended:

- This project focused on further developing an existing comprehensive biomass particle combustion model. The knowledge and capability gained from this project is used to improve the combustion behavior of industrial biomass suspension burners. The simplified particle model considering intra particle heat/mass transfer can be implemented in CFD simulation of a biomass suspension burner and a baseline model can be established to control the conversion process and burnout.

- In the current experimental study, due to the limited equipment, only the conversion time in different stages (ignition, devolatilization and burnout) were collected. Measuring the particle mass loss and particle temperature profile make the study much more robust.

- In this study, due to the lack of information about the irregularly shaped samples (collected from DONG Energy), a TG analysis was conducted to compare the conversion behavior of the samples with the behaviore of known pine wood. Due to the similarity of their characteristics, kinetics data of pine wood were applied for the irregularly shaped samples. For further study, it will be good idea to measure the reaction rates directly for the samples by TG analysis.

- Having much more complete data about irregularly shaped samples, as it was suggested above, helps to investigate and discuss the effects of milling process on the conversion chracteristcs of particles much more precise.

REFERENCES

Abbas, T., Costen, P., Kandamby, N.H., Lockwood, F.C., Ou, J.J., 1994. The influence of burner injection mode on pulverized coal and biomass cofired flames. Combustion and Flame. 99, 617-625.

Abbas, T., Costen, P.G., Lockwood, F.C., 1996. Solid fuel utilization: From coal to biomass. Symposium (International) on Combustion. 26, (2), 3041–3058.

Backreedy, R.I., Fletcher, L.M., Jones, J.M., Ma, L., Pourkashanian, M., Williams, A., 2005. Co-firing pulverized coal and biomass: a modeling approach. Proceedings of the Combustion Institute. 30, 2955–2964.

Balat, M., Ayar, G., 2005. Biomass energy in the world, use of biomass and potential trends. Energy Sources. 27, 931–940.

Bharadwaj, A., Baxter, L. L., Robinson, A. L., 2004. Effects of intraparticle heat and mass transfer on biomass devolatilization: experimental results and model predictions. Energy and Fuels. 18, 1021–103.

Blondeau, J., Jeanmart, H., 2011. Biomass pyrolysis in pulverized-fuel boilers: Derivation of apparent kinetic parameters for inclusion in CFD codes. Proceedings of the Combustion Institute. 3(2), 1787–1794.

Bryden, K. M. and Hagge, M. J., 2003. Modeling the combined impact of moisture and char shrinkage on the pyrolysis of a biomass particle. Fuel. 82, 1633-1644.

Chan, W.C. R., Kelbon, M., Krieger, B. B., 1985. Modeling and experimental verification of physical and chemical processes during pyrolysis of a large biomass particle. Fuel. 64, (11), 1505-1513.

Chen, Y., Mori, S., Pan, W., 1996. Studying the mechanisms of ignition of coal particles by TG-DTA. Thermochimica Acta. 275, 149-158.

Ciolkosz, D., 2010. Co-firing Biomass with Coal-Renewable and alternative energy fact sheet. The Pennsylvania State University.http://pubs.cas.psu.edu/freepubs/pdfs/ub044.pdf

Damstedt, B., Pedersen, J.M., Hansen, D., Knighton, T., Jones, J., Christensen, C., Baxter, L., Tree, D., 2007. Biomass cofiring impacts on flame structure and emissions. Proceedings of the Combustion Institute. 31, 2813-2820.

Demyirbas, A., 2003. Hydrocarbons from Pyrolysis and Hydrolysis Processes of Biomass. Energy Sources. 25, 67-75.

Di Blasi, C., 1993. Analysis of convection and secondary reaction effects within porous solid fuels undergoing pyrolysis. Combustion Science and Technology. 90, 315-340.

Di Blasi, C., 1996. Kinetic and heat transfer control in the slow and flash pyrolysis of solids. Industrial and Engineering Chemistry Research. 35, 37–47.

Di Blasi, C., 1996a. Heat, Momentum and Mass Transport through a Shrinking Biomass Particle Exposed to Thermal Radiation. Chemical Engineering Science. 51, (7), 1121-1132.

Di Blasi, C., 2000. Dynamic behavior of stratified downdraft gasifiers. Chemical Engineering Science. 55, 2931–2944.

Di Blasi, C., 2002. Modeling intra- and extra-particle processes of wood fast pyrolysis. American Institute of Chemical Engineers. 48, 2386–2397.

Di Blasi, C., Branca, C., 2001. Kinetics of primary product formation from wood pyrolysis. Industrial and Engineering Chemistry Research. 40, 5547–5556.

Di Blasi, C., Buonanno, F., Branca, C., 1999. Reactivities of some biomass chars in air. Carbon. 37, 1227-1238.

Essenhigh, R.H., Misra, M.K., Shaw, D.W., 1989. Ignition of coal particles: a review. Combustion and Flame. 77, 3-30.

Esteban, L. S., Carrasco, J. E., 2006. Evaluation of different strategies for pulverization of forest biomasses. Powder Technology. 166, 139–151.

Evans, R. J. and Milne, T. A. , 1987a. Molecular Characterization of the Pyrolysis of Biomass. 1. Fundamentals. Energy and Fuels. 1, (2), 123-137.

Evans, R. J. and Milne, T. A., 1987b . Molecular Characterization of the Pyrolysis of Biomass. 2. Applications. Energy and Fuels. 1, (4), 311-319.

Faúndez, J., Arenillas, A., Rubiera, F., García, X., Gordon, A.L., Pis, J.J., 2005. Ignition behavior of different rank coals in an entrained flow reactor. Fuel. 84, 2172-2177.

Forest Products Laboratory United States Department of Agriculture Forest Service, 1999. Chapter 3, Physical Properties and Moisture Relations of Wood, Wood Handbook: Wood as an Engineering Material, Madison, Wisconsin, Forest Products Society, 3-5.

Grieco, E. and Baldi, G., 2011. Analysis and modeling of wood pyrolysis. Chemical Engineering Science. 66, 650–660.

Gronli, M. G., Melaaen, M.C., 2000. Mathematical model for wood pyrolysis-comparison of experimental measurements with model predictions. Energy and Fuels 14,791–800.

Grotkjær, T., Johansen, K., Jensen, A., Glarborg, P., 2003. An experimental study of biomass ignition. Fuel. 82, 825-833.

Gubba, S.R., Ingham, D.B., Larsen, K.J., Ma, L., Pourkashanian, M., Tan, H.Z., Williams, A., Zhou, H., 2012. Numerical modelling of the co-firing of pulverised coal and straw in a 300 MWe tangentially fired boiler. Fuel Processing Technology. In Press.

Haseli, Y., Van Oijen, J.A., De Goey, L.P.H., 2011. A detailed one-dimensional model of combustion of a woody biomass particle. Bioresource Technology. 102, 9772–9782.

Haseli, Y., Van Oijen, J.A., De Goey, L.P.H., 2011. Numerical study of the conversion time of single pyrolyzing biomass particles at high heating conditions. Chemical Engineering Journal. 169, 299–312.

Jiménez, S., Remacha, P., Ballesteros, J.C., Giménez, A., Ballester, J., 2008. Kinetics of devolatilization and oxidation of a pulverized biomass in an entrained flow reactor under realistic combustion conditions. Combustion and Flame. 152, 588-603.

Karlström, O., Brink, A., Biagini, E., Hupa, M., Tognotti, L., 2012. Comparing reaction orders of anthracite chars with bituminous coal chars at high temperature oxidation conditions. Proceedings of the Combustion Institute. In Press, http://dx.doi.org/10.1016/j.proci.2012.07.011.

Koufopanos, C. A., Papayannakos, N., Maschio, G., Lucchesi, A., 1991. Modelling of the Pyrolysis of Biomass Particles. Studies on Kinetics, Thermal and Heat Transfer Effects. The Canadian Journal of Chemical Engineering. 69, (4), 907-915.

Kuo, J.T., Hsi, C.L., 2005. Pyrolysis and ignition of single wooden spheres heated in high-temperature streams of air. Combustion and Flame. 142, 401-412.

Larfeldt, J., Leckner, B., Melaaen, M. C., 2000. Modeling and measurements of the pyrolysis of large wood particles. Fuel. 70, 1637–1643.

Li, J., Brzdekiewicz, A., Yang, W., Blasiak, W., 2012. Co-firing based on biomass torrefaction in a pulverized coal boiler with aim of 100% fuel switching. Applied Energy. 99, 344–354.

Liden, C. K., Berruti, F., Scott, D. S., 1988. A kinetic model for the production of liquids from the flash pyrolysis of biomass. Chemical Engineering Communications. 65, 207-221.

Liliedahl, T., Sjöström, K., 1998. Heat transfer controlled pyrolysis kinetics of a biomass slab, rod or sphere. Biomass and Bioenergy. 15, 503-509.

Lu, G., Yan, Y., Cornwell, S., Whitehousem M., Riley, G., 2008. Impact of co-firing coal and biomass on flame characteristics and stability. Fuel. 87, 1133-1140.

Lu, H., 2006. Experimental and modeling investigations of biomass particle combustion. PhD Thesis, Brigham Young University.

Lu, H., Baxter, L., 2011. Biomass Combustion Characteristics and Implications for Renewable Energy. Green Energy and Technology. 95-12.

Lu, H., Ip, E., Scott, J., Foster, P., Vickers, M., Baxter, L.L., 2010. Effects of particle shape and size on devolatilization of biomass particle. Fuel. 89, 1156–1168.

Lu, H., Robert, W., Peirce, G., Ripa, B., Baxter, L., 2008. Comprehensive Study of Biomass Particle Combustion. Energy and Fuels. 22, 2826–2839.

Ma, L., Gharebaghi, M., Porter, R., Pourkashanian, M., Jones, J.M., Williams, A., 2009. Modelling methods for co-fired pulverised fuel furnaces. Fuel. 88, 2448–2454.

Ma, L., Jones, J.M., Pourkashanian, M., Williams, A., 2007. Modelling the combustion of pulverized biomass in an industrial combustion test furnace. Fuel. 86, 1959–1965.

Mandø, M., Rosendahl, L., Yin, C., Sørensen, H., 2010. Pulverized straw combustion in a low-NOx multifuel burner: Modeling the transition from coal to straw. Fuel. 89, 3051-3062.

Mania, S., Tabila, L. G., Sokhansanj, S., 2004. Grinding performance and physical properties of wheat and barley straws,corn stover and switchgrass. Biomass and Bioenergy. 27, 339 – 352.

Mehrabian, R., Zahirovic, S., Scharler, R., Obernberger, I., Kleditzsch, S., Wirtz, S., Scherer, V., Lu, H., Baxter, L. L., 2012. A CFD model for thermal conversion of thermally thick biomass particles. Fuel Processing Technology. 95, 96-108.

Patankar, S.V., 1980. Numerical heat transfer and fluid flow. Hemisphere Publishing Corporation.

Perry, R.H., Green, D.W., 1997. Perry's Chemical Engineers' Handbook (7th ed). McGraw-Hill.

Porteiro, J., Miguez, J.L., Granada, E., Moran, J.C., 2006. Mathematical modeling of the combustion of a single wood particle. Fuel Processing Technology. 87, 169-175.

Ragland, K. W. and Aerts, D. J., 1991. Properties of Wood for Combustion Analysis. Bioresource Technology. 37, 161-168.

Saastamoinen, J., Aho, M., Moilanen, A., Sørensen, L.H., Clausen, S., Berg, M., 2010. Burnout of pulverized biomass particles in large scale boiler – Single particle model approach. Biomass and Bioenergy. 34, 728-736.

Sadhukhan, A.K., Gupta, P., Saha, R.K., 2009. Modelling of pyrolysis of larg wood particle. Biosource Technology. 100, 3134-3139.

Sami, M., Annamalai, K., Wooldridge, M., 2001. Co-firing of coal and biomass fuel blends. Progress in Energy and Combustion Science. 27, 171-214.

Shaddix, C.R., Molina, A., 2009. Particle imaging of ignition and devolatilization of pulverized coal during oxy-fuel combustion. Proceedings of the Combustion Institute. 32, 2091-2098.

Spliethoff, H., Hein, K.R.G.,1998. Effect of co-combustion of biomass on emissions in pulverized fuel furnaces. Fuel Processing Technology. 54, 189-205.

Thunman, H., Niklasson, F., Johnsson, F., Leckner, B., 2001. Composition of volatile gases and thermochemical properties of wood for modeling of fixed or fluidized beds. Energy and Fuels 15, 1488–1497.

Thurner, F., Mann, U., 1981. Kinetic investigation of wood pyrolysis. Industrial and Engineering Chemistry Process Design and Development. 20, 482–488.

Wang, C., Wang, F., Yang, Q., Liang, R., 2009. Thermogravimetric studies of the behavior of wheat straw with added coal during combustion. Biomass and Bioenergy. 33, 50-56.

Wendt, C., Eigenbrod, C., Moriue, O., Rath, H.J., 2002. A model for devolatilization and ignition of an axisymmetric coal particle. Proceedings of the Combustion Institute. 29, 449-457.

Wornat, M.J., Hurt, R.H., Davis, K.A., Yang, N.C., 1996. Single-particle combustion of two biomass chars. Twenty-Sixth Symposium (International) on Combustion/The Combustion Institute. 3075-3083

Yang, Y.B., Sharifi, V.N., Swithenbank, J., Ma, L., Darvell, L.I., Jones, J.M., Pourkashanian, M., Williams, A., 2008. Combustion of a single particle of biomass. Energy and Fuels. 22, 306-316.

Yin, C., Kær, S.K., Rosendahl, L., Hvid, S.L., 2010. Co-firing straw with coal in a swirl-stabilized dual-feed burner: Modelling and experimental validation. Bioresource Technology. 101, 4169–4178.

Yin, C., Rosendahl, L., Kær, S.K., Condra, T.J., 2004. Use of numerical modeling in design for co-fring biomass in wall-fired burners. Chemical Engineering Science. 59, 3281 – 3292.

Yin, C., Rosendahl, L., Kær, S.K., Sørensen, H., 2003. Modelling the motion of cylindrical particles in a non-uniform flow. Chemical Engineering Science. 58, 3489 – 3498.

Yin., C., 2012. Microwave-assisted pyrolysis of biomass for liquid biofuels production. Bioresource Technology. 120, 273-284.

Zhang, D.K., Wall, T.F., 1994. Ignition of coal particles: the influence of experimental technique. Fuel. 73, 1114-1119.